

Andreas Borst

# Acid etching steel substrate pre-treatment for the physical vapor coating deposition





# Acid etching steel substrate pre-treatment for the physical vapor coating deposition process

By

Andreas Borst

in partial fulfilment of the requirements for the degree of

**Master of Science**

in Mechanical Engineering

at the Delft University of Technology,

to be defended publicly on Tuesday August the 22, 2018 at 14:00 AM.

Supervisor:	Dr. ir. W. G. Sloof
Thesis committee:	Prof. dr. ir. J. M. C. Mol, TU Delft
	Dr. Y. You, TU Delft
	Dr. R. J. Westerwaal, Tata Steel Europe

An electronic version of this thesis is available at <http://repository.tudelft.nl/>.

## ABSTRACT

---

In recent years, Tata Steel Europe has increased their focus on Physical Vapor Deposition (PVD) for the zinc coating application of their steel substrates, as an alternative to Hot Dip Galvanizing (HDG). PVD offers some benefits over HDG like multilayer structures and lower heat impact on the steel. To achieve sufficient coating adhesion strength of the zinc coating, before deposition the steel substrate is normally cleaned and activated by a plasma sputter unit. As this sputtering takes place in the vacuum chamber, like the deposition, it is prone to precipitation of sputtered material in the vacuum chamber. If the PVD process is scaled up to an industrial coating line, the volumes of sputtered material and precipitated material will become problematic for the service reliability. Therefore it has been investigated whether an acid etching surface pre-treatment step before the vacuum chamber could reduce the needed plasma intensity, and thereby decrease the sputtered volume in the vacuum chamber.

A range of acid etching times and plasma sputtering times were tested, to obtain the range in which the coating adhesion was sufficient. To test the coating adhesion, two (automotive) tests were used. It was found that by pickling, the plasma sputter intensity could not be reduced. So the coating adhesion strength seemed not directly related to the pickling time, for the particular steel used in this project.

After the limits of good adhesion were determined, the characterization started to identify what in the elemental composition or the surface morphology could determine whether there was good adhesion or not. It was found that (even very short) pickling completely removes the surface enrichment of the first 50 nm, while plasma sputtering only lowers the surface enrichments. It was found that plasma sputtering does not influence the morphology, while pickling smoothens the surface out, with increasing pickling. As the oxygen concentration profile did not change significantly as function of pickling time, but its enrichment thickness was about equal to the minimum plasma sputter depth, it is thought that the oxygen concentration is the major influence on good and bad adhesion.

## ACKNOWLEDGMENTS

---

I would like to take this opportunity to thank those who have supported, guided and encouraged me through this project. That is primarily Dr. Ruud Westerwaal, my daily supervisor at Tata Steel, and Dr. Wim Sloof, as my university supervisor. I am obliged great thanks to you both for the patient and encouraging way of guiding me through the project; Ruud Westerwaal especially for having multiple fruitful discussions together, being always available to help out and your many hours of reading and improving my thesis. Wim Sloof for his support and feedback on the project and thesis, and also for the Auger characterization he carried out.

I also really enjoyed the time at Tata in IJmuiden, thanks to the PVD team (Erwin, Colin, Christiaan) for their support, input, discussions and daily fun and laughter together, the pickling guys (Piet, Jacques), those who helped with characterization (Erdni, Hans). Also special thanks to Kees (TU Delft) who helped me greatly by carrying out XPS tests and by teaching me how to analyze the XPS results. He also helped out a lot to improve my SEM images.

# CONTENTS

---

Abstract.....	4
Acknowledgments.....	5
1 Introduction.....	7
1.1 Tata Steel / IJmuiden plant.....	7
1.2 Physical vapor deposition.....	8
1.3 Project.....	9
2 Relevant background information.....	12
2.1 Pickling.....	12
2.2 Plasma sputtering.....	13
2.3 Oxidation at low temperatures.....	15
2.4 Interface adhesion.....	17
3 Experimental setup and procedures.....	18
3.1 Characterization techniques.....	18
3.2 Substrate material.....	21
3.3 Surface treatment.....	22
3.4 Coating deposition.....	24
3.5 Adhesion test procedures.....	25
4 Results.....	26
4.1 Coating adhesion results.....	26
4.2 Microstructural characterization of coatings with OK adhesion.....	30
4.3 Microstructural characterization of coatings with NOK adhesion.....	32
4.4 Morphological characterization of pickled steel.....	33
4.5 Characterization of the steel surface by Auger Electron Spectroscopy.....	36
4.6 GDOES characterization.....	38
4.7 XPS characterization.....	46
5 Discussion.....	48
5.1 Influence of re-oxidation.....	48
5.2 Manganese oxide.....	49
5.3 Influence of plasma sputtering on the steel surface state.....	50
5.4 Coating adhesion influencing factors.....	51
6 Conclusions.....	52
6.1 Recommendations.....	53
7 References.....	54

# 1 INTRODUCTION

---

## 1.1 TATA STEEL / IJMUIDEN PLANT

The steelmaking plant in IJmuiden is part of Tata Steel Europe. Around 9000 people work at the plant in IJmuiden, and produce more than 7 million tons of high-quality steel every year. The steel is mostly used in automotive, building and packaging industries. Other applications are batteries, tubes and industrial vehicles. Beside steel coils, Tata Steel offers also design, consultancy and technology services to their customers.

The majority of the steel strip sold by Tata Steel to the automotive market is coated with a Zn or ZnAlMg coating for corrosion protection. Such coatings are most often deposited using a Hot Dip Galvanising (HDG) or electro plating (EZ<sup>1</sup>) process. However, these processes suffer from de-wetting (HDG) (Langkruis, et al., 2015) and hydrogen embrittlement (EZ) (Hillier & Robinson, 2004). Therefore Tata Steel works on the development of a novel Physical Vapor Deposition (PVD) technology for the deposition of coatings onto high strength steels (HSS).

---

<sup>1</sup> EZ: Electrolytic Zinc.

## 1.2 PHYSICAL VAPOR DEPOSITION

Physical Vapor Deposition (PVD) is a coating process in which atoms or molecules of a material are vaporized by heating a solid or liquid source, and transported in the form of a vapor through a vacuum or low-pressure gaseous environment, and condenses on a cold substrate. PVD processes can be used to deposit films of elemental, alloy, and compound materials as well as some polymeric materials. Typically, PVD processes are used to deposit films with a thickness range of nanometers to micrometers. Typical PVD deposition rates vary from 1-10 nm/sec (Mattox, 2001), but can be significantly higher at elevated temperatures, to for example a micron per second<sup>2</sup>. The coatings can consist of a single or multilayer structure whereas every layer can consist of a single or multi element composition.

Tata has 2 PVD setups at the R&D lab, named Emely and Betsy. For this project, only Emely was used.

---

<sup>2</sup> Observed at Tata test setup.

## 1.3 PROJECT

### 1.3.1 Problem

High-strength steels are often coated with a zinc layer for protection against corrosion. Normally, the coating is applied by Hot Dip Galvanizing (HDG), where the steel strip is dipped into a molten zinc bath. However, this procedure has some disadvantages, especially now that the steels and the coating requirements get more advanced, for example by enhancing their microstructure. Some disadvantages are:

- The high temperature of the zinc bath, approximately 460 °C, which does influence the microstructure and thus the desired properties of the steel.
- The inability to apply more than one coating layer.
- Surface wetting for high strength steels can be problematic.

To be able to coat Advanced High Strength Steels (AHSS), another coating technique was proposed, namely PVD. With this technique, the coating is applied by condensation of a zinc vapor on the steel surface. This technique does eliminate some of the difficulties of HDG, but has some challenges of its own. The cleaning and surface preparation of the steel before vapor deposition is vital to obtain good coating adhesion. This treatment is normally done by plasma sputtering of the steel, which does remove the top layer of the substrate and consists of an oxide layer and elemental enrichments. The plasma sputtering will also increase the temperature of the steel substrate. Previous research at Tata showed that there is a minimum substrate temperature for achieving good<sup>3</sup> coating adhesion (Maalman, Vlot, & Zoestbergen, 2011).

The plasma sputtering seems to be vital to get good coating adhesion. However the amount of residue removed by the plasma will result in difficulties for an industrial PVD coating line; the residue precipitates, especially in the sputter unit. This could be countered by either reducing the residue volume, or by directing most of the residue to a preferred, easily maintainable location in the vacuum chamber.

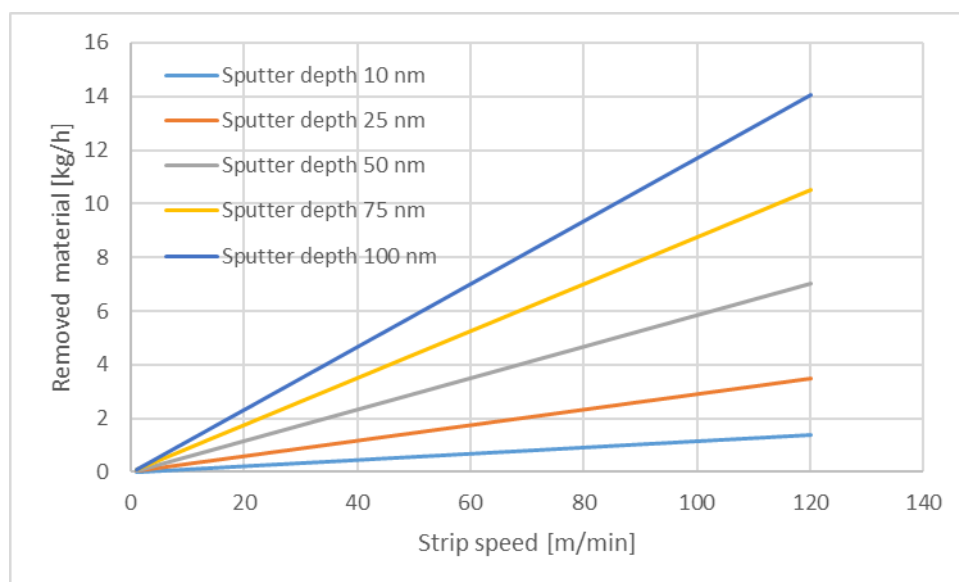


Figure 1: Calculated removed material vs strip speed for various sputter depths

<sup>3</sup> Good adhesion is when the specimen obeys two industrial adhesion tests, as explained in section 3.5.

To make an estimation of the impact of the residue volume in the vacuum chamber on an industrial coating line, a calculation was made. As strip width 1.75 m was taken and the sputtered residue mass was calculated as function of strip speed and sputter layer thickness. The results are shown in Figure 1. It can be seen that the volume is in the order of kilograms per hour, which does not allow continuous coating deposition.

### 1.3.2 Aim of the project

The background of this project is to reduce the residue volume removed by the sputter unit by adding a pickling pre-treatment step. If the pickling process removes partially or completely the oxide layer, then the plasma sputter intensity<sup>4</sup> and the amount of residue can be reduced. Therefore in this research the interplay between acid etching and subsequent plasma cleaning is investigated. In the limiting case, where a very low plasma cleaning intensity is used (i.e. = low substrate temperature), an additional infrared heating step is included to compensate.

### 1.3.3 Research questions

This research seeks answers to the following questions:

1. Can, by using acid etching pre-treatment, the sputter intensity be reduced, and thereby extend the runtime of the PVD process?
2. What are the key parameters for the acid etching process?
3. What is the difference in surface condition in terms of morphology and composition after pickling and after plasma cleaning?

### 1.3.4 Challenges

The challenge of this research is to arrange the steel surface pre-treatment steps in such a way that the plasma cleaning step of the PVD process can be reduced to a minimum. This will imply that the surface oxides and enrichments need to be reduced to a sufficient low value which enables good coating adhesion properties, while at the same time minimize the re-oxidation and contamination effects between the different steps. Furthermore, all process steps must be performed in such a way that differences are minimized and thus also the spread in experimental results.

The re-oxidation between process steps is a significant challenge; in an industrial coating line, the time between pickling and coating deposition will at maximum be 10 s, with the high strip speeds normally used. In this project, the pickling setup and the coating deposition setup were in different labs, so there was at least 30 min time between pickling and coating deposition. It is expected that this re-oxidation time will have significant influence on the results.

### 1.3.5 Structure of the thesis

In this thesis, a brief summary of relevant process information is given in Chapter 2. In Chapter 3, the setups for all the experimental work are described, together with the procedures, characterization techniques and material used. In Chapter 4, the results for both the adhesion tests and the characterization of the substrate are presented. In Chapter 5, these results are discussed, as to understand the underlying mechanisms. Finally, the conclusions are given in Chapter 6.

---

<sup>4</sup> Plasma sputter intensity is controlled by the power and sputter time.

## 2 RELEVANT BACKGROUND INFORMATION

---

*This chapter will address briefly the relevant information of techniques and processes used in the experimental work.*

### 2.1 PICKLING

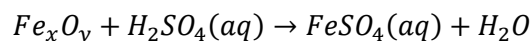
For most industrial pickling purposes either sulfuric acid or hydrochloric acid is used. Both are strong acids, but there is a difference in reactivity and kinetics for various substrates. In this chapter, the focus will be on sulfuric acid pickling and its mechanism on the iron oxide and substrate. The alloying elements, which also form oxides, do also need to be considered. If there is preferential pickling or enrichment at the surface due to pickling, the characterization in Section 4.6 will reveal that.

#### 2.1.1 Aim of pickling

Pickling is tried as a pre-treatment step because it can remove the oxide layer, and possibly also the surface enrichments. The cleaned substrate could then potentially be sputtered by lower plasma sputter intensities, without losing adhesion strength.

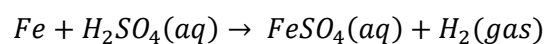
#### 2.1.2 Pickling mechanism

There are 3 common iron oxides expected at the surface of the substrate; ferrous oxide (Wüstite, FeO), magnetic iron oxide (magnetite, Fe<sub>3</sub>O<sub>4</sub>), and ferric oxide (hematite, Fe<sub>2</sub>O<sub>3</sub>, often the outermost layer). The reactions of the iron oxide with the sulfuric acid are:



The iron sulfate will stay in solution and gives the solution after some time a brownish color.

As the iron oxide is removed from the surface, the sulfuric acid will get in direct contact with the steel substrate. This is mainly metallic iron and then the major reaction will be:



When the steel substrate was immersed longer than 20 seconds in the acidic bath<sup>5</sup>, a gas was observed bubbling from the surface into the solution. It is expected that this is the hydrogen gas resulting from the pickling of metallic iron. This suggests that (under these test conditions) after around 20 seconds, the acid has removed most of the oxide layer, or at least partially reached the metallic iron. It is noted that no pickling inhibitor was used during these experiments.

---

<sup>5</sup>Solution composition: sulfuric acid 50gr/l; temperature: 25 °C. Rest of the acid bath properties given in Section 3.3.1.

## 2.2 PLASMA SPUTTERING

Plasma is called the fourth state of matter (Liebermann & Lichtenberg, 2005), i.e. when atoms decompose (often) from a gas into freely moving charged particles. Plasmas have several applications like deposition, etching, light production and electrical conduction.

Plasma sputtering is used to remove the oxide layer, the surface enrichments and to activate the surface. This is a vital step to achieve a good coating adhesion. For this plasma sputter process argon is often used, which is a relatively heavy and noble element. A heavy element is beneficial for the efficiency of the sputtering; a noble element is needed to prevent possible chemical reactions with steel.

Plasma is a gas composed of charged atoms. Over longer ranges, these charges 'cancel' each other, therefore plasma is a quasi-neutral gas. These moving charged particles induce magnetic fields in the plasma.

Electrons do leave their atom when there is sufficient strong electric field. This leaves 2 charged particles, an ion and an electron. After the plasma is initiated, the 'free' electrons assist the ionization process by collisions with argon atoms. The electrons will also recombine with the argon ions into neutral atoms and with the side walls of the plasma sputter unit.

### 2.2.1 Sputter yield

In the sputtering process, an argon ion bombards the substrate, removing atoms from the surface. The ratio of sputtered metallic atoms over the amount of incoming argon ions is called the "yield". The higher the yield, the more efficient the plasma is. The yield increases with voltage difference and is also related to the angle of the incoming argon ions.

It is expected that the yield depends on the atomic weight of the target nucleus. In Table 1, the weight of nucleuses is given of elements that are expected to be involved in the sputtering. The weight is taken as the amount of neutrons and protons of the most occurring isotope on earth.

If the atomic number of the target ( $Z_t$ ) and incident ions ( $Z_i$ ) both are large and not too different, that is

$$0,2 \leq Z_t/Z_i \leq 5$$

and

$$Z_t, Z_i \gg 1$$

Then the sputtering yield,  $\gamma_{sput}$ , can be estimated with the following empirical formulae (Liebermann & Lichtenberg, 2005) and (Zalm, 1984):

$$\gamma_{sput} \approx \frac{0.06}{\varepsilon_t} \sqrt{\bar{Z}_t} (\sqrt{\varepsilon_i} - \sqrt{\varepsilon_{thr}})$$

with

$$\bar{Z}_t = \frac{2 Z_t}{(Z_i/Z_t)^{2/3} + (Z_t/Z_i)^{2/3}}$$

The mean energy  $\varepsilon_t$  is the surface binding energy, given in Table 1. The mean energy of the incident argon ions  $\varepsilon_i$  is given by the applied voltage. The surface binding energy is taken as the enthalpy of formation, which is a simplification (Liebermann & Lichtenberg, 2005).

The mass (in amu) of the incoming ion is  $M_i$ , the mass of the target ions is  $M_t$ . If  $M_i/M_t > 0.3$  then from (Bohdansky, 1980) an expression for  $\varepsilon_{thr}$  is obtained;

$$\varepsilon_{thr} \approx 8\varepsilon_t \left( \frac{M_i}{M_t} \right)^{2/5}$$

If the voltage difference is set at 400 V<sup>6</sup>, then the sputter yields for several elements could be calculated. It can be seen in Table 1 that the yield does vary over a rather large range. It is therefore expected that preferential sputtering can occur, and that enrichments of carbon and silicon can be anticipated due to the plasma sputtering. In section 4.6, this hypothesis will be tested.

Element	Nucleus weight	Atomic number	Surface binding energy	Relative sputter yield
	<i>amu</i>		<i>eV</i>	
Mn	55	25	2.29	2.0
Cu	63	29	3.53	1.3
Fe	56	26	3.52	1.3
Cr	52	24	3.59	1.2
Al	27	13	3.42	0.8
Si	28	14	4.72	0.6
C	12	6	7.43	0.1

Table 1: Calculated relative sputter yield for several elements, sorted on the sputter yield

It has been determined experimentally that the plasma sputtering in Emely has a rate between 0.15 and 0.35 nm/s (Westerwaal, Commandeur, & Bouwens, 2017) - when using comparable conditions as in this project<sup>7</sup>.

<sup>6</sup> The power supply used is mostly in the range of 400-500V. The supply is controlled at 200W.

<sup>7</sup> For example 200 W plasma power, DP800 substrate.

### 2.3 OXIDATION AT LOW TEMPERATURES

For this project, only low-temperature oxidation is relevant, with temperatures at about room temperature. The re-oxidation between pickling and coating deposition is important, since in this project there is a non-negligible time in between pickling and sputtering during which the substrate is exposed to atmospheric air. The amount or order of magnitude of this re-oxidation should be known, to account for it in the results.

The rate of oxidation at low temperatures has been modelled by (Martin & Fromm, 1997), as function of several parameters. This model will be used in this thesis to investigate the rate of re-oxidation after pickling.

After the first monolayer formation the oxide growth requires oxygen transport through the oxide (or metal transport the other way). At these temperatures, diffusion is too slow for the observed oxide growth. The model is used to explain what then the rate determining influence is.

The model assumed a contact potential between the metal and the adsorbed oxygen at the oxide surface. This potential difference formed across the thickness of the oxide scale is called the Mott potential. The oxygen or metal atoms migrate as charged defects through the oxide lattice. The transport of these defects is enhanced by the Mott field<sup>8</sup>, and thus, a detectable oxide skin can grow, even at room temperature.

Figure 2 shows the Mott potential and the oxide thickness (oxygen absorption expressed in monolayers oxygen) as function of time, for various temperatures. The lower part of the graph shows the Mott potential only; the top part shows the oxide growth.

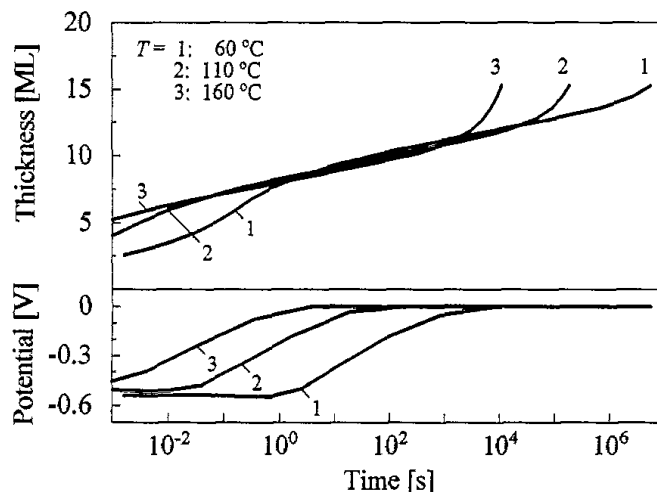


Figure 2: Calculated influence of temperature on the oxide growth (Martin & Fromm, 1997)

In this project, the average transfer time in ambient atmosphere between acid etching and deposition is on the order of hours. From Figure 2 it can be seen that the typical oxide thickness is around 12 monolayers. The acid etching is carried out at room temperature, so from this figure, a re-oxidation thickness of 12 monolayers is expected. This should probably be removed by the plasma sputtering just before deposition.

<sup>8</sup> As the oxide thickness is in the range of nanometers, the electric field can be very high, although the potential is in the order of 0.5 V.

From the figure it can be seen that the temperature in this temperature range is only of significance after about  $10^4$  seconds, which is about 1 hour. It is noted that the effect of temperature for exposure times less than 1 s is not relevant for our research. The temperature however will be room temperature until it enters the vacuum chamber of Emely. This implies that for our conditions the oxide layer grows logarithmically with time.

It is expected that the concentration of water vapor has a significant influence on the oxidation of the steel specimen, but in literature not much on this topic could be found for oxidation at room temperature, except that water vapor will increase oxidation.

## 2.4 INTERFACE ADHESION

The adhesion of a metallic coating on a steel surface depends on:

1. Work of adhesion at the interface needed to separate the coating from the substrate (Song & Sloof, Characterization of the failure behavior of zinc coating on dual phase steel under tensile deformation, 2011)
2. Internal stresses in the coating (Song, Sloof, Pei, & de Hosson, 2006), which increase with increasing coating thickness
3. Ductility of the coating (Song & Sloof, Characterization of the failure behavior of zinc coating on dual phase steel under tensile deformation, 2011)

Low substrate temperatures result in a smaller grain size of the coating layer. For pure zinc deposition, the temperature should be above 140 °C, in order to achieve good adhesion (Maalman, Vlot, & Zoestbergen, 2011). Below that temperature, no good adhesion was observed.

Micro cracks in the coating layer at the interface with steel may be induced by the thermal residual stress due to the large difference in coefficient of thermal expansion between the zinc coating and steel substrate when the sample was cooled from the melting point of zinc (419 °C) to room temperature (~20 °C). These micro cracks weaken the zinc grain boundaries. (Song & Sloof, Characterization of the failure behavior of zinc coating on dual phase steel under tensile deformation, 2011) To investigate the influence of the thermal expansion differences between steel and zinc, some calculations have been made in Section 4.2.1 to determine its significance.

### 3 EXPERIMENTAL SETUP AND PROCEDURES

*In this chapter the most significant parts of the experimental work and experimental setups will be explained.*

#### 3.1 CHARACTERIZATION TECHNIQUES

To analyse the effect of pickling on the adhesion of the coating, several techniques were used. Each technique, discussed below in more detail, provides information about the chemical composition/state at various depths of the sample; see Figure 3.

##### 3.1.1 SEM

Scanning Electron Microscopy (SEM) is a characterization technique that images the sample surface by scanning it with a high-energy beam of electrons in a raster like pattern. The electrons interact with the sample at and close to the surface (up to a few 100 nm). Secondary and backscattered electrons are detected, each provide different information as they are the results of different interactions (see below). In combination with energy dispersive X-ray spectroscopy (EDX), information about the sample's surface topography and chemical composition is provided.

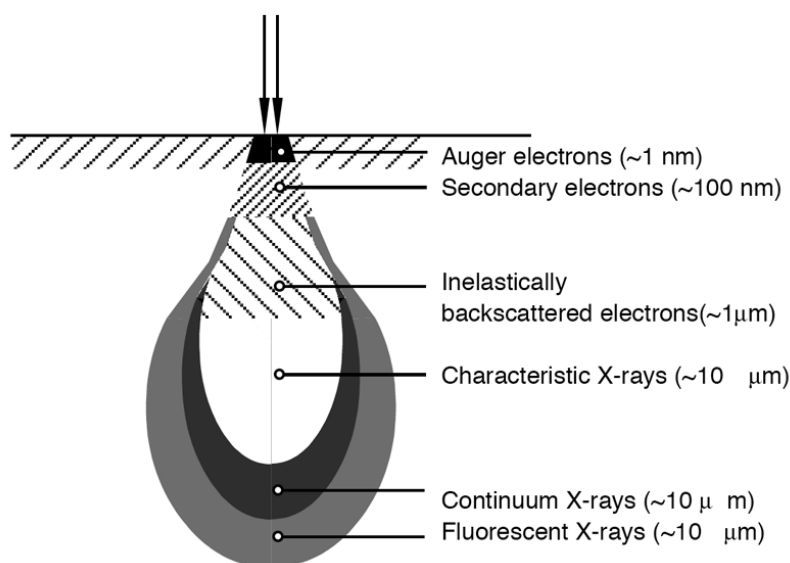


*Figure 3: Schematic of the interaction volume of Scanning Electron Microscopy<sup>9</sup>*

##### 3.1.2 SEM - Secondary electrons

Secondary electrons are the result of electron emission of surface atoms, initiated by the inelastic collisions with the 'primary' high-energy electrons. These secondary electrons have a low energy, and require a mean free path to escape from the sample. Only for the top few nm of the sample, the secondary electrons are unaffected. Therefore, secondary electrons provide information about the morphology of the sample.

<sup>9</sup> Image from <https://sites.ualberta.ca/~ccwj/teaching/microscopy/>

### 3.1.3 SEM - Backscattered electrons

Backscattered electrons are reflected 'primary' electrons, which have elastically collided with the atoms. These electrons provide information about the composition of the sample. As the backscattered electrons have a higher energy than secondary electrons, they provide compositional information up to 100 nm from the surface. In such an image, the (average) kinetic energy of the elements is displayed as function of brightness: heavier elements will occur brighter than light elements.

### 3.1.4 SEM - Energy dispersive X-ray spectroscopy

Often, SEM imaging is combined with energy dispersive X-ray spectroscopy (EDX). EDX is a technique to determine the elemental composition of the sample surface. EDX is based on the interaction of the 'primary' electrons with atoms, with the emission of X-rays as a result. As each element has a unique electron structure, the wavelength of the emitted X-rays is a characteristic of the element. EDX provides compositional information up to  $\sim 1 \mu\text{m}$ .

### 3.1.5 Auger electron spectroscopy

Auger electron spectroscopy (AES) is a technique to analyze the surface in great detail. Auger electrons are the result of internal relaxation steps of excited/ionized atoms. Atoms that are excited/ionized atoms due to the interaction with 'primary' electrons, can release photons due to the relaxation of electrons within the atom. Although the energy of these photons is low, it can be enough to induce the ionization of atoms and to produce so-called Auger electrons. Auger electrons have energies specific for each element, ideal for compositional analysis. However, their energy is low. Therefore, their mean free path is also small and only the first few nm of the sample surface can be analyzed by means of AES.

### 3.1.6 XPS

X-ray Photoelectron Spectroscopy is a technique to study the composition and chemical state of elements in the top few nanometers of the sample surface. The sample is irradiated with a beam of X-rays of known energy, which is often Mg  $K\alpha$  (1253.6 eV) or Al  $K\alpha$  (1486.6 eV). The photons are able to excite electrons with sufficient energy to escape its orbit. In this way, the kinetic energy of the electrons provides information about the composition and chemical state (bonding). XPS does not discriminate the same elements, if their bonding, or oxidation state, is different.

However, this information is lost when the electrons collide within the sample. Therefore, only the electrons from the top few nanometers of the sample have a free path to the detector. Depth information can be obtained by the combination with etching techniques, although this destroys the sample. The analysis depth is a few nanometers, but it can be combined with etching techniques to get a concentration-depth profile.

### 3.1.7 GDOES

GDOES is a destructive technique that is used to obtain the elemental composition of the sample as function of the depth, up to 100  $\mu\text{m}$ . It combines plasma sputtering and electron excitation and relaxation for element detection. During analysis argon plasma is generated by applying a voltage

between anode and cathode, which is the sample. Ionized argon atoms are accelerated towards the sample. As a result, the sample surface is bombarded and surface atoms will be sputtered from the sample. These sputtered atoms are excited in the plasma and upon relaxation (de-excitement). They will emit photons with a characteristic wavelength. The amount and the wavelength of the photons are then used to determine the composition of the sputtered layer. Knowing the sputter rate, the detection of the photons as a function of time provides a composition-depth profile of the sample.

### 3.2 SUBSTRATE MATERIAL

The steel specimens used for these projects' experiments are taken from DP800<sup>10</sup> steel, with a thickness of 1.0 mm. These were cut into plates of 178x112 mm which are subsequently numbered individually. The composition of the DP800 steel was determined by GDOES as given in Table 2. The tensile strength was also tested in three directions, relative to the rolling direction. Every direction was tested three times and averaged results are given in Table 3.

Element	Composition
	<i>wt%</i>
Iron	Bal.
Manganese	1.90
Chromium	0.59
Silicon	0.30
Carbon	0.15
Aluminium	0.05
Titanium	0.04

Table 2: Steel substrate composition, based on GDOES characterization

Direction relative to rolling direction	E modulus	Yield strength	Ultimate tensile strength
	<i>GPa</i>	<i>MPa</i>	<i>MPa</i>
Longitudinal	188	498	820
Transverse	215	493	840
Diagonal (45°)	195	472	803

Table 3: Steel substrate mechanical properties, based on 9 tensile tests

---

<sup>10</sup> DP800: Dual Phase steel combines both strength and ductility; 800 is an indication for the ultimate tensile strength in MPa.

### 3.3 SURFACE TREATMENT

#### 3.3.1 Pickling

The aim of the project is to see whether pickling can reduce the plasma sputter intensity while maintaining good coating adhesion properties. Pickling is often used to remove surface oxides and surface enrichments.

Prior to the acid etching an electroplating cleaning procedure was applied. First the steel is manually degreased with acetone and anodically cleaned in a sodium hydroxide bath at 60 °C for 1 minute. In between anodic cleaning and pickling the plates were rinsed with demi water. Then, the acid etching is performed with times between 0 and 5 minutes. It was observed that after around 20 to 30 seconds in the acid bath, bubbles start to form at the steel surface, due to the reaction with the iron substrate, as described in Section 2.1. After pickling the steel is again rinsed with demi water. To reduce the brownish colored film over the substrates after drying, probably due to some residual sulfuric acid, an additional cleaning step was applied using a sodium hydroxide bath. In this bath the residual sulfuric acid reacts with sodium hydroxide. This left the sodium hydroxide bath with a brownish color, but it does remove most of the brown haze on the steel plates. The sodium hydroxide does not react with the steel. All the bath parameters are given in Table 4.

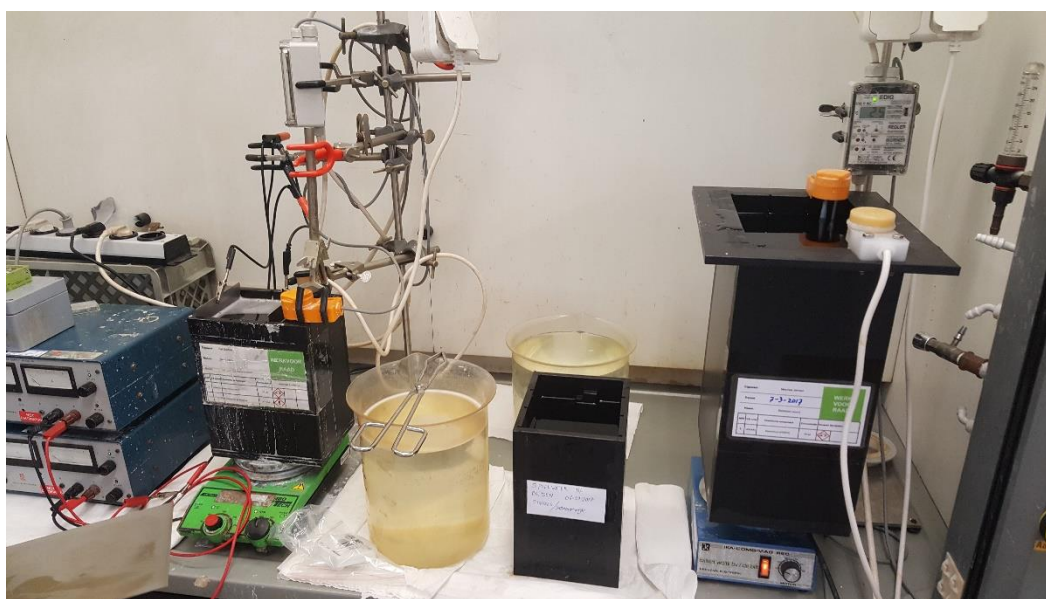


Figure 4: Photograph of the pickling setup, from left to right: Power supply, cathodic sodium hydroxide bath, demi water bath after cathodic cleaning, demi water bath after pickling, sulfuric acid bath

Process parameters	Anodic cleaning	Etching
Solution composition	27 g/l NaOH 8.1 ml/l Unisurfa KB 35 Additive	50 g/l H <sub>2</sub> SO <sub>4</sub> (96%)
Temperature	60 °C	25 °C
Current Density	+1.5 (anodic)	0 (dip)
Time	60	various

Table 4: Process parameters of the alkaline and sulfuric acid baths

### 3.3.2 Infrared heating

IR heating could be used to compensate for the low substrate temperature when low plasma sputter intensities are used. If infrared heating was applied, it is used in the PVD vacuum chamber of Emely. The infrared lamp does radiate its heat on the backside of the steel substrates. The infrared lamp was operated with a power in the range of 600-700 W, and applied for times in the range of 2 to 10 minutes. Substrate temperatures were measured, with maxima of around 200 °C after 10 minutes by only infrared heating.

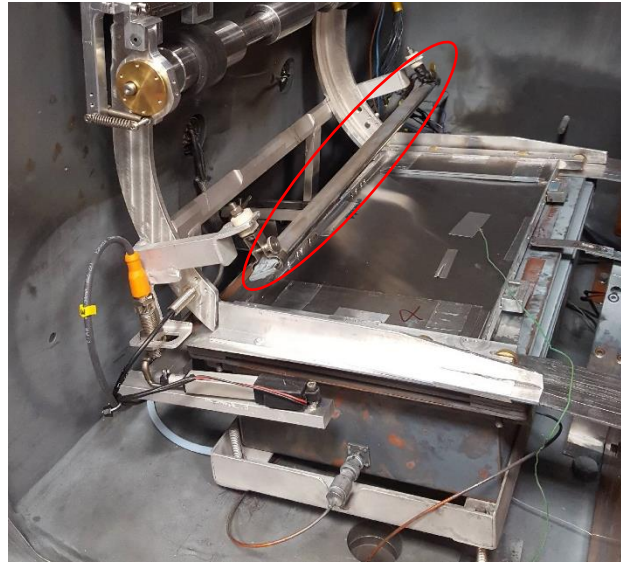


Figure 5: Photograph of the sputter unit in Emely with infrared heating unit (in red) installed and sample cart ready for test

### 3.3.3 Plasma sputtering

The plasma sputter unit, as can be seen in Figure 5, is placed in front of the Vapor Deposition Box (VDB) to clean, activate and heat up the substrate before coating deposition at the VDB. The plasma sputter unit is slightly tilted with respect to the steel strip to decouple the plasma sputter process from the transport strip of Emely. The plasma sputter unit consists of two copper boxes and bars with permanent magnets in the inner box. The positive potential is applied to the inner box, while the outer box is grounded. Due to the voltage difference electrons are created by gas ionization. The electrons are trapped in the magnetic field around the magnetic bars and move in a direction perpendicular to the electric and magnetic field. This results in a spiral-like motion along the magnet bars. The electron cloud near the magnet bars assists the ionization of the argon gas. The positive argon ions move away from the electron cloud and the anode inner box. This results in an increased concentration of ionized argon atoms close to the steel sheet and thus in an increased sputter intensity. The argon gas flow is controlled via an inlet valve, but kept mostly constant throughout this project at 323 sccm. The temperature of the steel specimen was measured with K-type thermocouples, which were spot welded onto the steel sheet surface to be sputtered.

Tests were carried out in Emely with typical plasma sputter times ranging from 1 to 6 minutes, with a sputter power of 200 W and an argon flow of 323 sccm<sup>11</sup>.

<sup>11</sup> sccm = standard cubic centimeters per minute.

### 3.4 COATING DEPOSITION

The coating deposition in the vacuum chamber starts by placing the steel substrates in the carts and inserting the carts in the vacuum chamber. Then the chamber is closed and pumped down to  $2 \times 10^{-4}$  mbar. When this vacuum pressure is reached, the vapor deposition box (VDB) is heated up to 900 °C and the zinc melt is heated up to 645 °C. When these conditions are reached, the steel surface treatment is applied, i.e. optional infrared heating and thereafter plasma sputter cleaning. After the surface treatment is finished, the cart is transported over the VDB with a strip speed of 1 m/min. Here the coating deposition takes place. When the cart has left the strip, the next cart is loaded, surface treatment is applied, and the cart is transported over the vapor deposition box. This procedure repeats until the last cart, if that cart is coating deposited as well the zinc melt and the VDB are cooled down. After cooling down the vacuum chamber can be opened and the carts can be taken out.

### 3.5 ADHESION TEST PROCEDURES

Two tests were executed to determine the zinc coating adhesion on steel, namely the so-called BMW adhesion test and the OT bending test.

The BMW adhesion test is developed to represent single layer zinc adhesion behavior under crash like conditions. The test does mechanically load the specimen, until failure of the adhesive. It is then observed whether the zinc coating is still attached to the steel substrate, or the zinc coating is attached to the adhesive. With sufficient coating adhesion strength, the coating should still stick to the steel substrate.

A line of adhesive<sup>12</sup> of around 100 mm length, about 4-5 mm thick and at least 10 mm wide is applied. Curing of the adhesive takes place in a furnace kept at 175 °C for 30 minutes. After cooling down, the strip is bent over more than 90° with the glue at the exterior. The glue breaks in this process. Any delamination of the zinc coating is observed visually with the naked eye and judged. If the metallic coating is completely removed from the substrate then the coating is qualified as Not OK (NOK). If the metallic coating stays intact and the adhesive fails, leaving some remnants onto the metallic coating, then the test result is qualified as OK. (Langkruis, Zoestbergen, & Maalman, Adhesion, forming and corrosion performance of multi layer Zn-Mg PVD coating systems for automotive applications, 2013).

The OT bending test is done without an additional adhesive; the steel substrate with a zinc coating is bended completely, until the back sides of the steel substrate touch each other. The zinc coating should be at the outer part of the bend. Duct tape is applied on the zinc coating at the bended side of the specimen. To investigate the adhesion, the duct tape is pulled off quickly. If the coating adhesion is OK, there will be no zinc visible on the duct tape. If there is zinc visible on the duct tape, the result is Not OK (NOK).

	<b>OK</b>	<b>Not OK</b>
<i>OT</i>	No (zinc) contamination visible on the duct tape	Zinc visible on the duct tape
<i>BMW</i>	No zinc coating visible on the epoxy	Zinc coating visible on the epoxy, steel spots or areas visible on the substrate

Table 5: Definitions for the BMW and OT adhesion test results

<sup>12</sup> Betamate 1496V of DOW Chemical

## 4 RESULTS

---

*In this chapter the coating adhesion test results and the subsequent characterization as carried out by XPS, GDOES and SEM (EDS) will be presented.*

### 4.1 COATING ADHESION RESULTS

For the coating adhesion experiments, the zinc-coated steel sheets were cut into specimen with dimensions of 25 by 112 mm. These specimens had a thickness of 1.0 mm and the zinc coating thickness was in the range between 4 and 15  $\mu\text{m}$ . Of each coated steel sample, 4 specimens were cut for the OT and BMW test, i.e. 3 specimens for the BMW test and 1 for the OT test. If not all results are OK and not all results are NOK, then the result is noted as OK/NOK. In Figures 6 and 7, tested specimens are shown, both OT and BMW test.

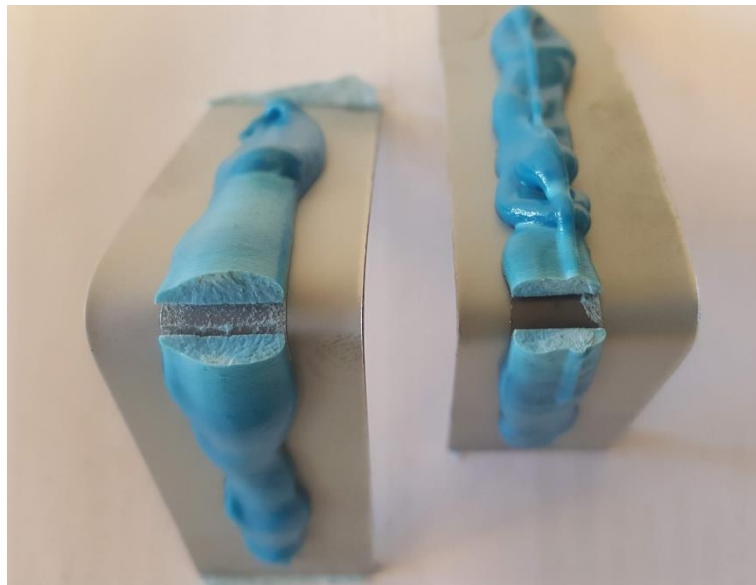


*Figure 6: BMW-tested specimens with OK (left) and NOK (right) adhesion*

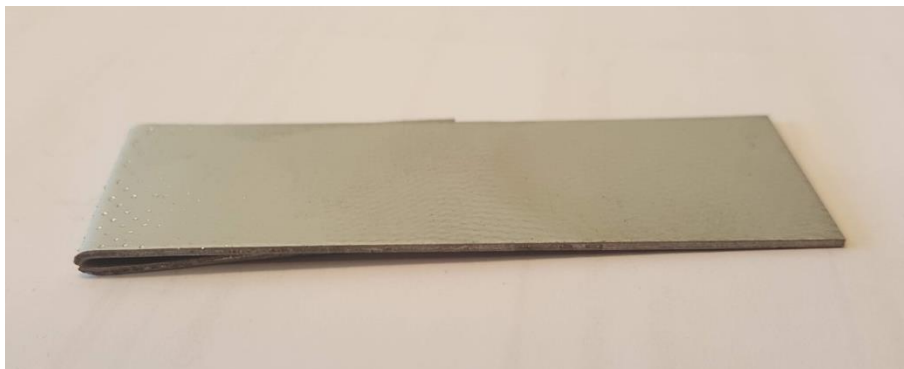


*Figure 7: OT-tested specimen, the tested side is on the left*

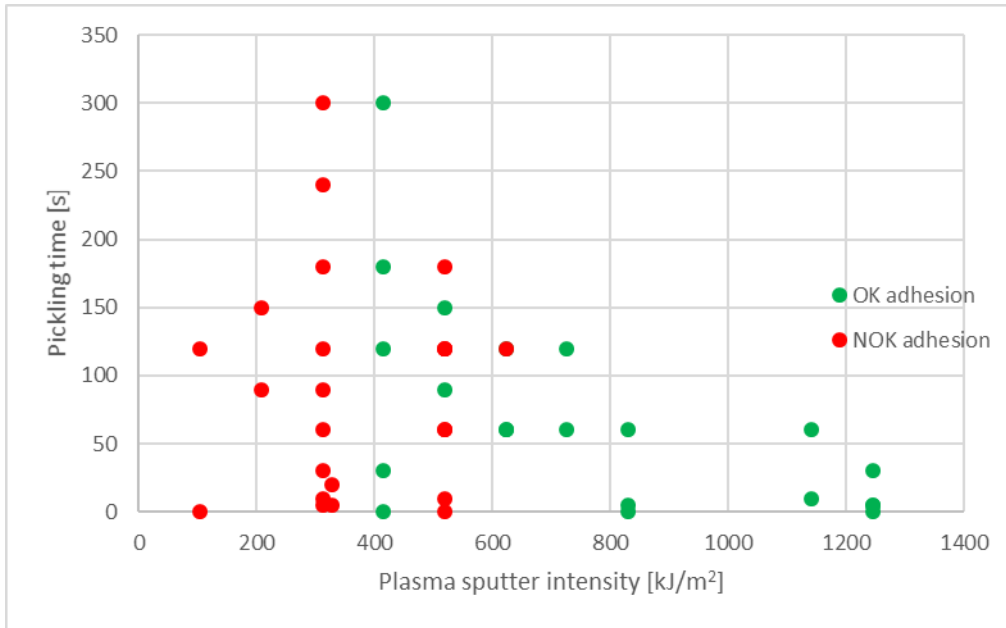


Figure 8: OT adhesion test results as function of pickling time and plasma sputter intensity

Figure 8 shows the OT adhesion test results as a function of plasma sputter intensity and pickling time. In green, the OK results are given, in red the Not OK results. Clearly it can be seen that below 400 kJ/m<sup>2</sup><sup>13</sup>, all the adhesion test results are NOT OK, even for long pickling times. At higher sputter intensities between 400 and 700 kJ/m<sup>2</sup> the results show the possibility of both OK and NOT OK adhesion results. Beyond the sputter intensity of 700 kJ/m<sup>2</sup><sup>14</sup> all results show OK adhesion, independent of the pickling time.

<sup>13</sup> 400 kJ/m<sup>2</sup> corresponds with approximately 2 minutes at 200W sputtering, which corresponds to a removed thickness of ~18 nm.

<sup>14</sup> 700 kJ/m<sup>2</sup> corresponds with approximately 3.5 minutes at 200W sputtering, which corresponds to a removed thickness of ~31.5 nm.

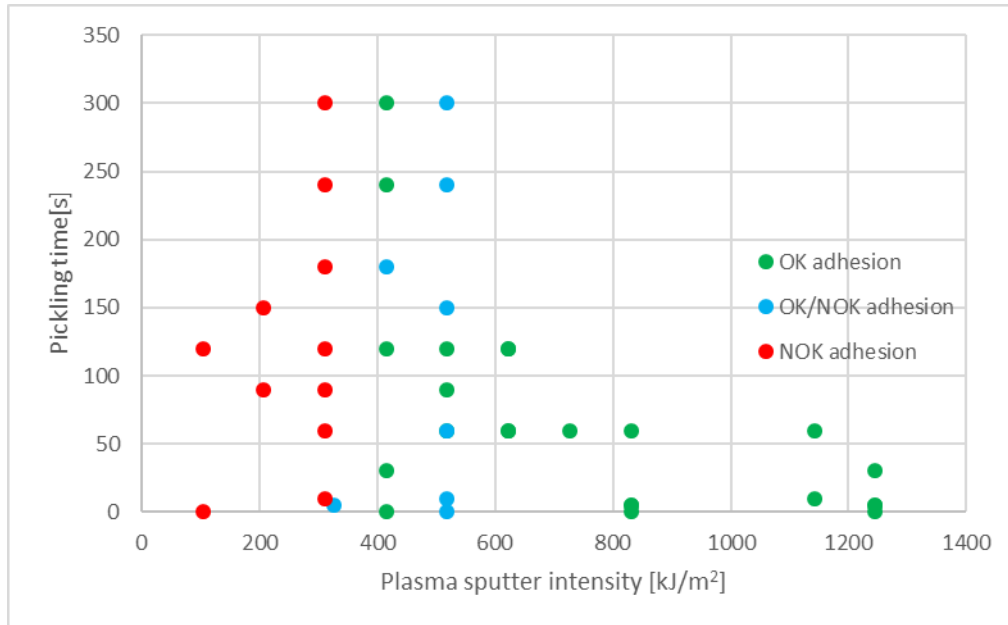


Figure 9: BMW adhesion test results as function of pickling time and plasma sputter intensity

Figure 9 shows a similar graph as in Figure 8, but now with the results of the coating BMW crash test. Each dot in the graph represents 3 BMW test results. If green, all 3 tests results were OK, if red all 3 test results were Not OK, if blue there was both OK and Not OK results. It can be seen that only for sputter intensities exceeding 400 kJ/m<sup>2</sup>, there can be good adhesion. For sputter intensities higher than 600 kJ/m<sup>2</sup>, all tests results showed good adhesion.

#### 4.1.1 IR assisted coating adhesion test results

Plasma sputtering does not only sputter away material from the surface, but it also heats up the substrate. Previous research indicated that if the steel substrate temperature is low<sup>15</sup>, the coating adhesion strength is reduced (Maalman, Vlot, & Zoestbergen, 2011). Especially for lower plasma sputter intensities, the coating adhesion might be influenced by this lower substrate temperature. This influence could possibly be a result of lower surface diffusion of zinc atoms at the interface. Therefore, the influence of IR pre-heating is investigated, in order to obtain a good coating adhesion with lower sputter intensity.

Insufficient adhesion typically starts from 320 kJ/m<sup>2</sup>. This equals plasma sputter times of 1.5 minutes. Therefore this sputter intensity is used for testing the IR heat assistance influence.

<sup>15</sup> That is below 144 °C for Zn coatings.

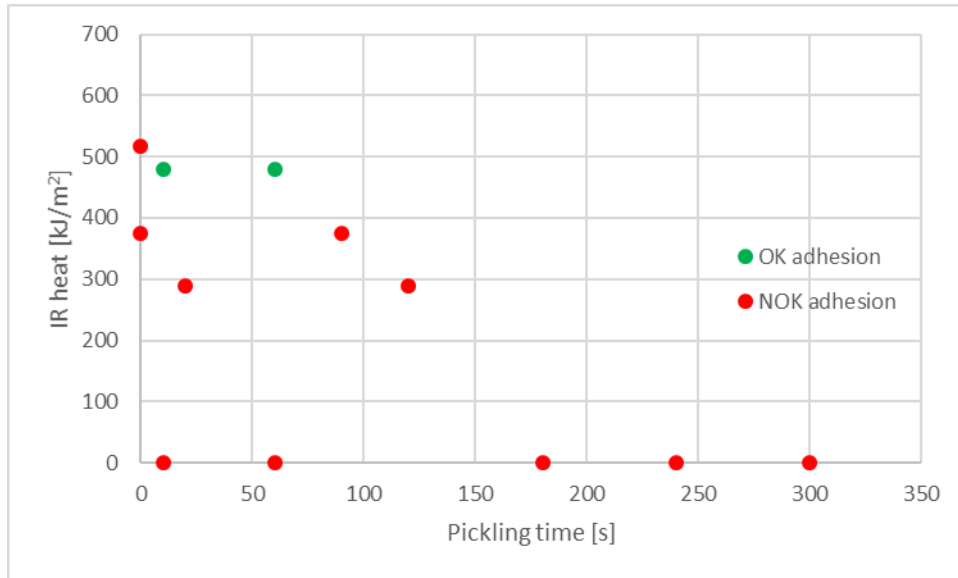


Figure 10: BMW adhesion test results at 1.5 min sputter time, with infrared heated samples (pickling time versus infrared heating intensity)

In Figure 10 the BMW coating adhesion results are given as function of IR heating and pickling time for a constant plasma sputter intensity of  $320 \text{ kJ/m}^2$ , where never good adhesion was observed. It shows mostly NOT OK adhesion results, which is to be expected for this sputter intensity, based on previous results; see Figures 8 and 9. There are two results, however, which show an OK adhesion. This is the case when IR heating is combined with an additional pickling step. This suggests that IR heating could assist the plasma sputtering to achieve good coating adhesion.

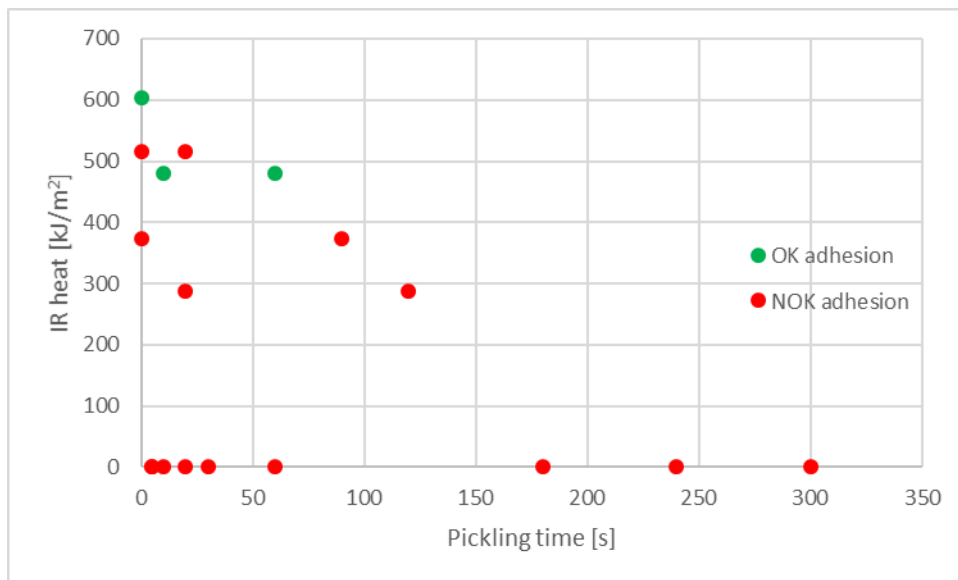


Figure 11: OT adhesion test results at 1.5 min sputter time, with infrared heated samples (pickling time versus infrared heating intensity)

In Figure 11 the OT coating adhesion results are given as function of IR heating and pickling time for a constant plasma sputter intensity of  $320 \text{ kJ/m}^2$ . It shows mostly Not OK adhesion. There are three results, however, which show an OK adhesion. This is the case when IR heating is increased above  $450 \text{ kJ/m}^2$ . This suggests that IR heating could assist the plasma sputtering to achieve good coating adhesion. Even for plasma sputter intensities which were not sufficient when combined with pickling, to get good adhesion.

## 4.2 MICROSTRUCTURAL CHARACTERIZATION OF COATINGS WITH OK ADHESION

To address why a coating performs OK or NOK during the adhesion tests, chemical and structural characterization analysis were performed. In this section, a structural characterization is presented of the coating with an OK coating adhesion test. In Figure 12, images of three BMW-tested cross-sections are shown, zoomed in on the zinc coating.

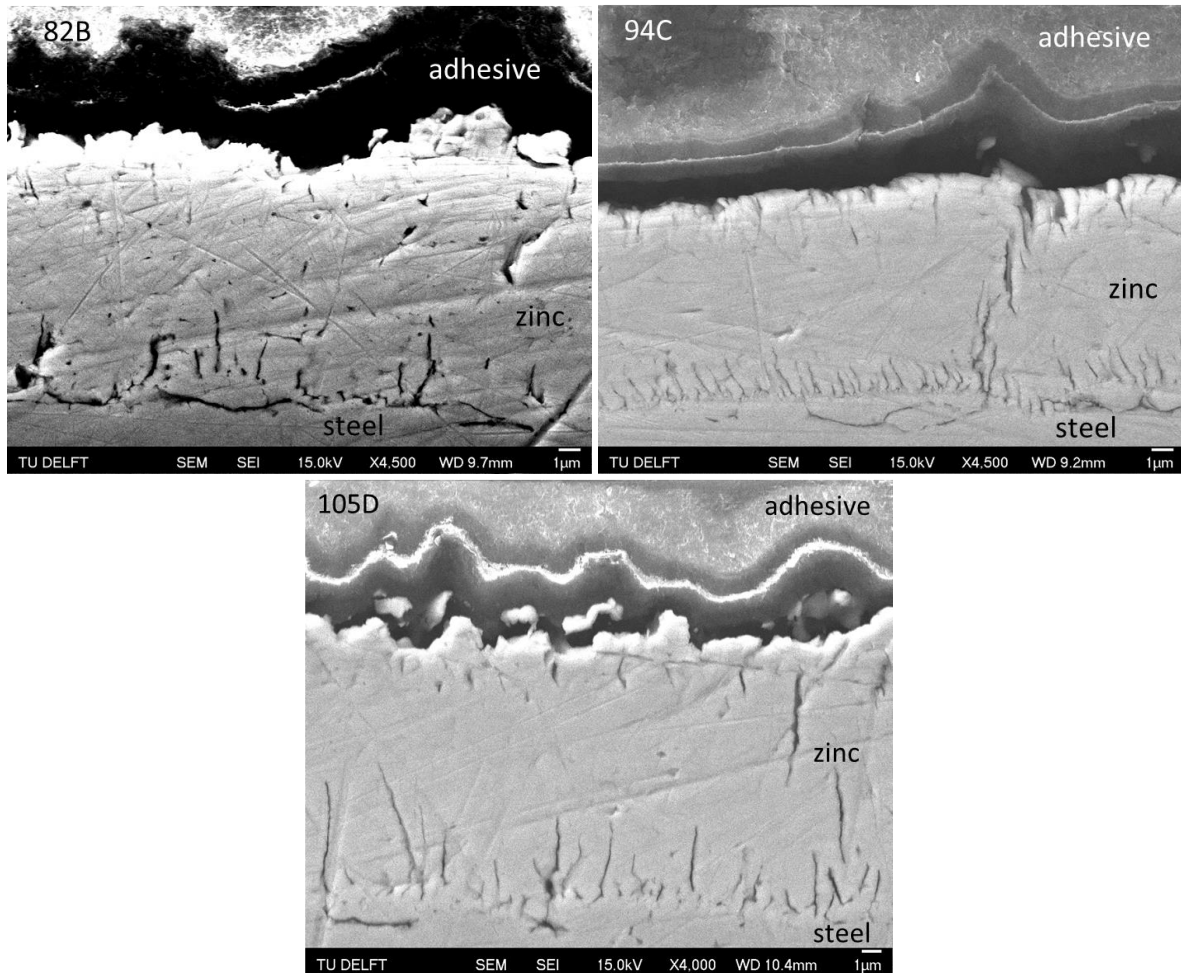


Figure 12: Cross-section images (SEM SE) of three BMW-tested specimens

	<b>82B</b>	<b>94C</b>	<b>105D</b>
Pickling	130 s	300 s	10 s
IR heating	150 °C	0 °C	150 °C
Plasma sputtering	42 kJ/m <sup>2</sup>	42 kJ/m <sup>2</sup>	31 kJ/m <sup>2</sup>
Coating thickness	9 µm	8 µm	13 µm

Table 6: Process parameters for samples 82B, 94C and 105D

The pre-treatment parameters for these samples are given in Table 6. The main difference in substrate preparation is in the pickling time and IR heating, while the sputter intensity is kept almost constant.

These SEM observations of the cross section of the zinc coatings (with OK adhesion) show in general a homogeneous coating layer structure with a comparable surface roughness. Remarkably, although the coating adhesion is good, all samples show at the steel zinc interface cracks, which run from the steel surface into the zinc. These types of cracks are also present at the zinc-adhesive interface.

These cracks might be caused by:

- The sample preparation procedure; the sample is cut, sawn, grinded and polished, and especially during the first 2 steps, cracks could initiate or propagate due to induced stresses.
- By stress effects in the coating; there is a temperature difference between the zinc vapor (~645 °C) and the steel substrate (max: 200 °C<sup>16</sup>). There is also a different coefficient of thermal expansion (CTE). Both the temperature difference and the different CTE's will induce stresses and can thereby initiate cracks. In the next section the potential influence of the thermal expansion will be investigated.

#### 4.2.1 Thermal misfit between zinc and steel

The linear coefficient of thermal expansion is for steel ~12  $\mu\text{m}/\text{m}^\circ\text{C}$ , for zinc ~28  $\mu\text{m}/\text{m}^\circ\text{C}$  (Callister, 2007). As the vapor is deposited on the steel substrate, it is still above its melting temperature. Only after solidification of the zinc, stresses can start to be induced by the thermal contraction. Zincs melting point is at ~420 °C, below that temperature the stresses can start to add up, since the zinc is solidified to the steel substrate. The temperature decreases until room temperature, which we set at 20°C for this calculation.

Two theoretical cases can be identified that can serve as boundaries for the maximum and minimum misfit;

1. Suppose that there is no temperature gradient in whole sample, then the whole specimen is at the same temperature. The stresses then come only from the difference in coefficient.
2. Suppose that the steel substrate is at 200 °C and cools down from there. Then the stresses between coating and substrate will be increased by the smaller temperature difference in the steel ( $\Delta T=200-20$  °C), compared to the temperature difference in the zinc coating ( $\Delta T=420-20$  °C).

The temperature difference and the contraction over this temperature difference in the steel and in the zinc can then be calculated for both cases. The results of this calculation are shown in Table 7.

	<b>Case 1</b>	<b>Case 2</b>
$\Delta T$ steel	400 °C	180 °C
$\Delta x$ steel	4.8 mm/m	2.1 mm/m
$\Delta T$ zinc	400 °C	400 °C
$\Delta x$ zinc	11.2 mm/m	11.2 mm/m
Misfit between zinc and steel	6.4 mm/m	9.1 mm/m

Table 7: Calculation of the thermal misfit due to contraction for steel and zinc

When the used specimen are considered, with length up to 178 mm, see Section 3.2, then the misfits between substrate and coating become 1.1 mm and 1.6 mm over this specimen length. These misfits can very well be the cause of the cracks at the interface between the steel substrate and the zinc coating.

<sup>16</sup> Substrate temperature was occasionally measured with a thermocouple.

### 4.3 MICROSTRUCTURAL CHARACTERIZATION OF COATINGS WITH NOK ADHESION

In this section, a structural characterization is presented of the coating with an NOK coating adhesion test. In Figure 13, images of two BMW-tested cross-sections are shown, zoomed in on the zinc coating.

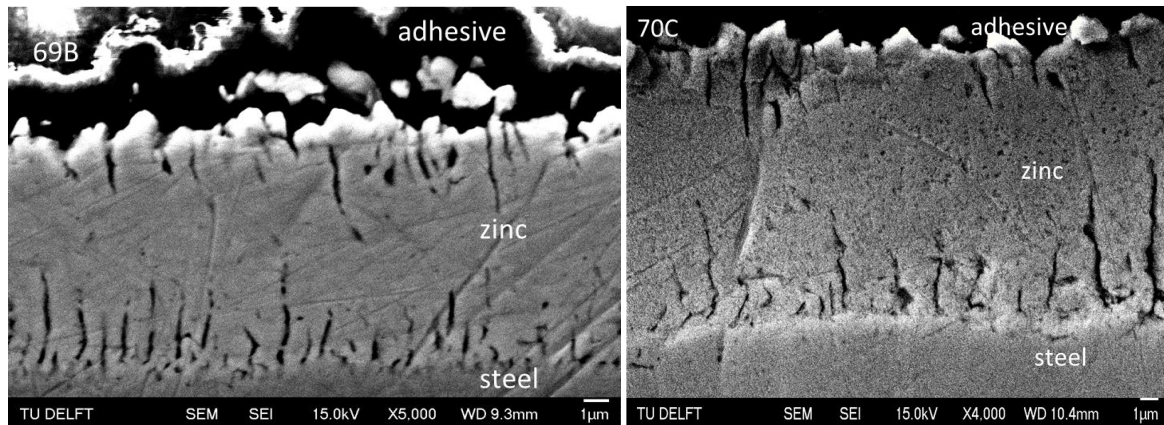


Figure 13: Cross-section images (SEM SE) of two BMW-tested specimens

	<b>69B</b>	<b>70C</b>
Pickling	180 s	60 s
IR heating	No	No
Plasma sputtering	1.5 min	1.5 min

Table 8: Process parameters for samples 69B and 70C

This SEM characterization of the cross section of the zinc coating with NOK adhesion shows some typical features. In all cases there seems to be (small) cracks at the interface between the steel surface and the zinc coating. Also at the interface between the zinc coating and the adhesive there seems to be cracks, however smaller in length and with a lower number of cracks. These cracks seem to be a bit more pronounced than in the case of the OK adhesion. On this scale, the influence of the differences in pre-treated of the steel substrate cannot be seen. What can be seen for both OK and NOK coatings is that there are cracks over the full thickness of the coating. However a clear indication for the difference in coating adhesion properties cannot be deduced from these SEM cross-section observations.

#### 4.4 MORPHOLOGICAL CHARACTERIZATION OF PICKLED STEEL

The morphology of the steel surface was analyzed with SEM to understand the influence of acid etching. Four samples<sup>17</sup> with parameters given in Table 9 were characterized.

Sample	Pickling time seconds
VII	0
XI	10
XII	20
XIII	30

Table 9: Pickling times of 4 samples

The samples were not pre-cleaned with cathodic cleaning, nor was there a sodium hydroxide bath afterwards. Sample VII was used as reference for the other samples, since it was only cleaned with ethanol.

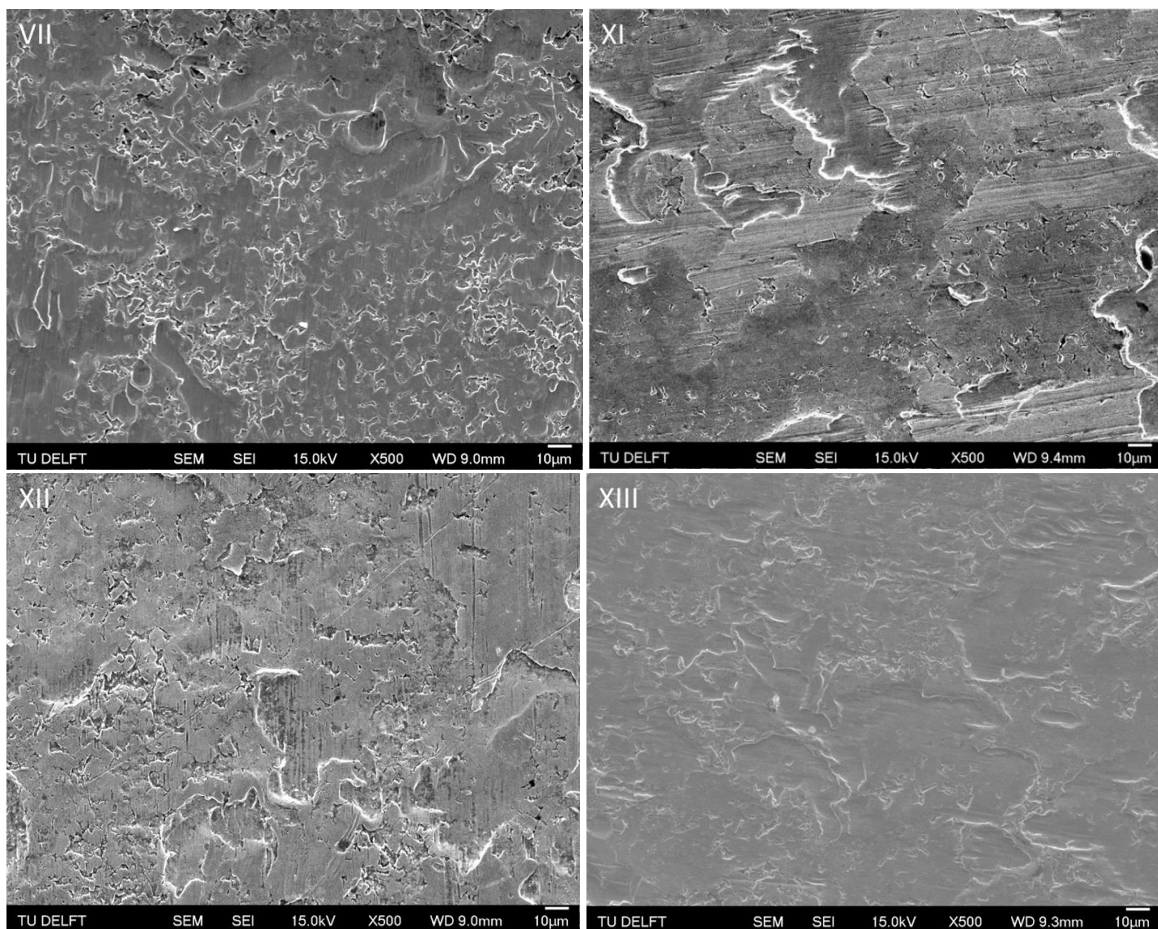
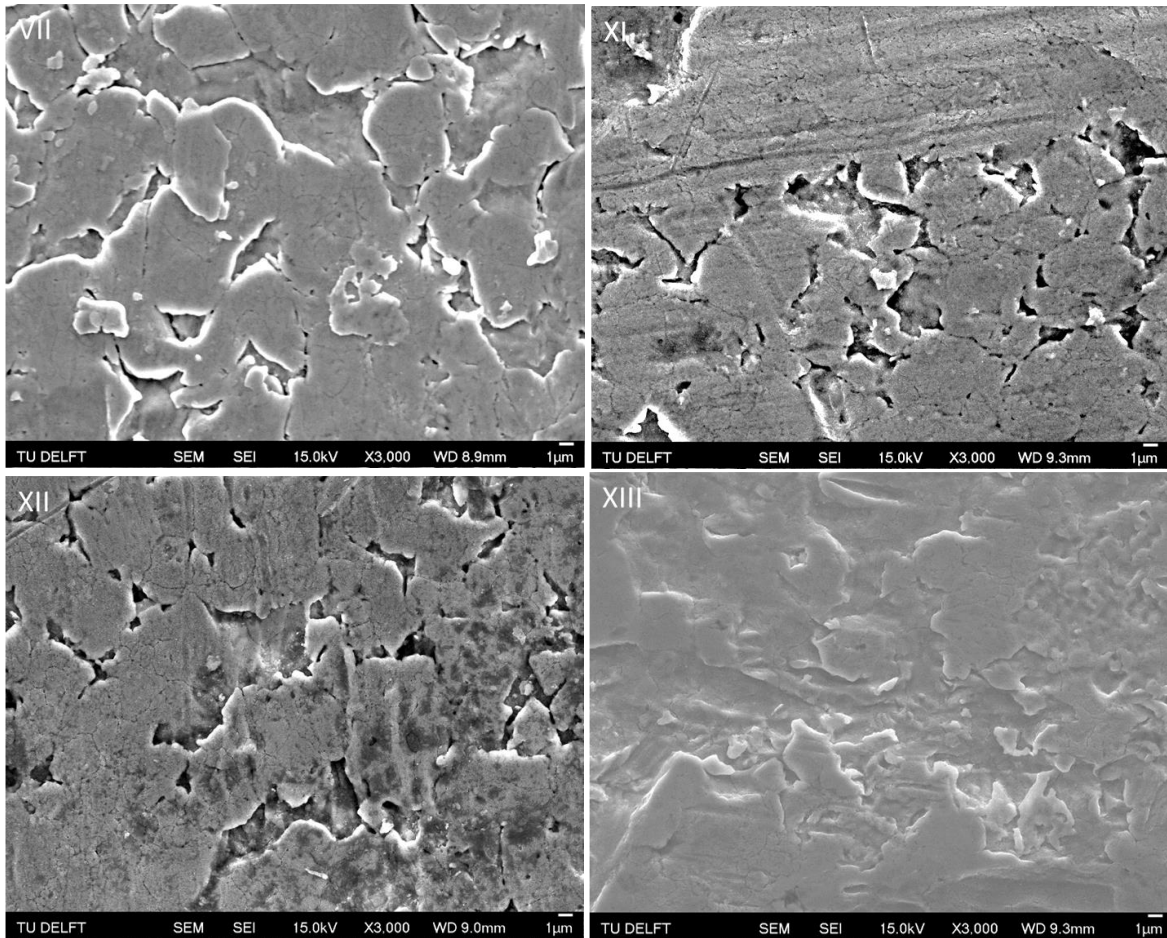


Figure 14: SEM topography images of pickled steel surface, magnification 500x

Figures 14, 15 and 16 show the morphology for various pickling times, in the range between 0 and 30 seconds, at different magnifications. It can be seen that at 30 seconds (XIII), the surface seems to smoothen out, creating a more even surface. This trend can already be seen for the 10 (XI) and 20 s (XII) pickling.

<sup>17</sup> Material taken from the same plates as all other samples.



*Figure 15: SEM images of pickled steel substrate, magnification 3000x*

At a magnification of 3000x, the grains of the substrate can clearly be distinguished. It can be seen that for increasing pickling the surface seems to flatten out.

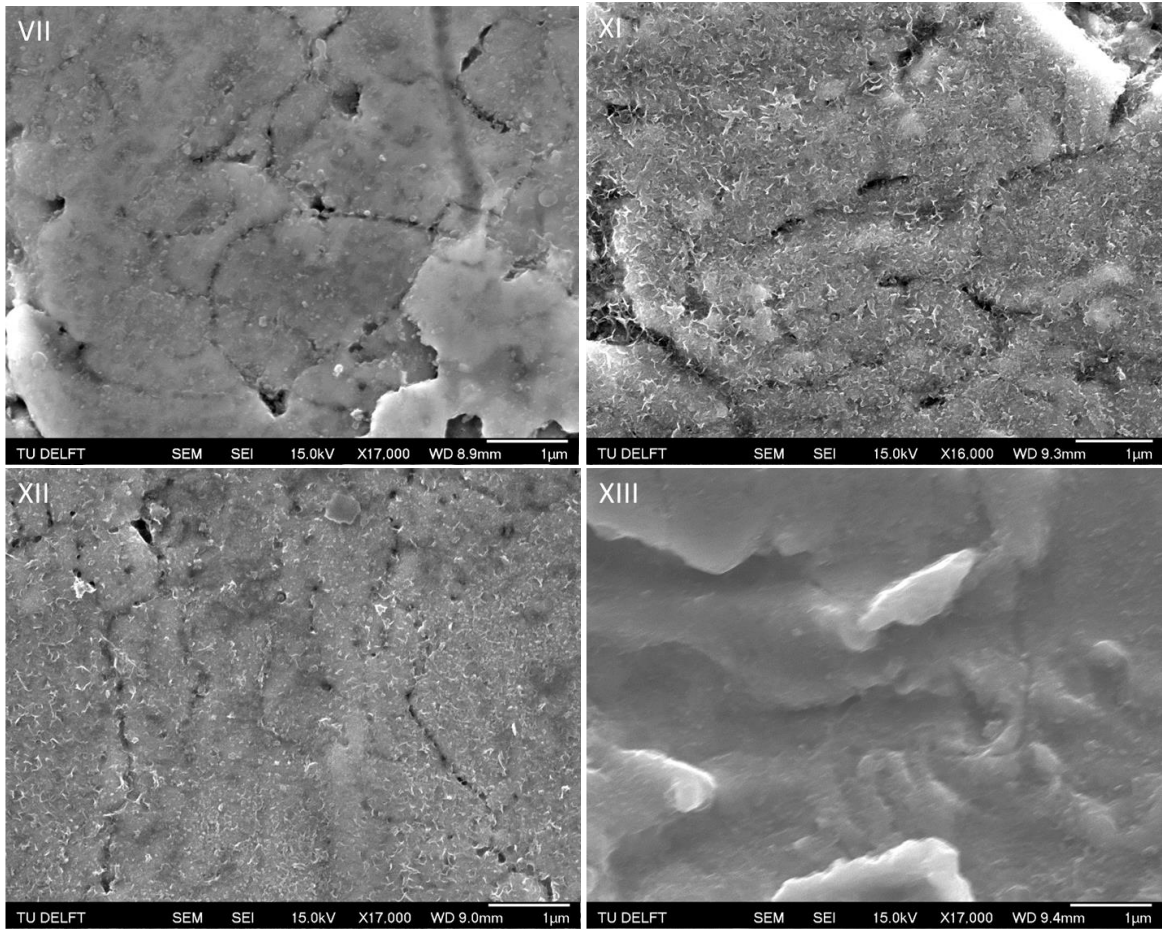


*Figure 16: SEM images of pickled steel substrate, magnification 16000-17000x*

At magnifications around 17000x, particles on the surface are visible in Figure 16. For 10 and 20 seconds pickling, these particles are distributed evenly and have sizes of around 100 nm in length. After 30 seconds pickling, there are no such particles visible. It is expected that these particles are left parts of oxides, which are etched away after 30 seconds.

#### 4.5 CHARACTERIZATION OF THE STEEL SURFACE BY AUGER ELECTRON SPECTROSCOPY

To investigate what determines the difference (morphology, composition) between an OK and NOK coating adhesion Auger Electron Spectroscopy (AES) was performed on the fractured surface after a BMW adhesion test. With this characterization, the elemental composition on the surface can be determined after delamination.

For this experiment two samples have been selected which show partial delamination of the coating after the BMW test. The coating adhesion strength for these samples is therefore expected to be at the transition between OK and NOK, i.e. a critical value. On these spots AES have been performed, see Figures 17 and 18.

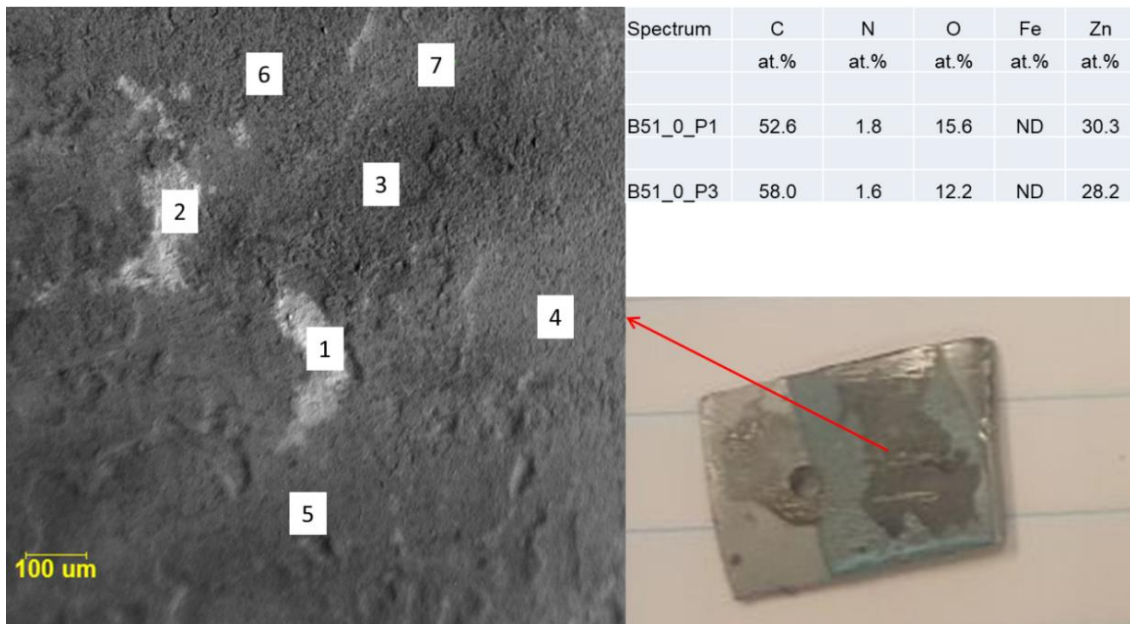


Figure 17: AES measurement of sample 51 on the fractured surface after the BMW adhesion test. The spots indicate the location of the AES acquisition.

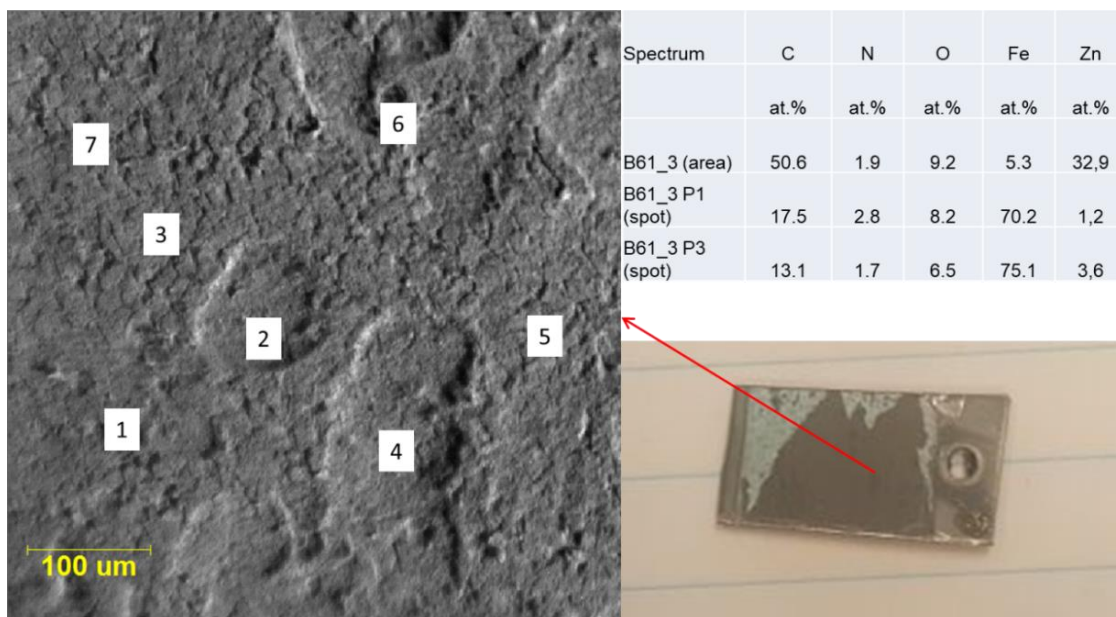


Figure 18: AES measurement of sample 61 on the fractured surface after the BMW adhesion test. The spots indicate the location of the AES acquisition.

These measurements indicate that in one case there is still a considerable amount of zinc present on the surface (51) while in the other case there is only a marginal amount of zinc remains on the surface (61), while both measurements were made at the steel surface, where the zinc delaminated from the steel substrate. The fact that in both cases there is still zinc on the surface (but not visible by the naked eye) might imply that the zinc layer ruptures in the zinc layer, just above the interface and thereby leaving zinc on the steel surface. This has also been seen in previous SEM EDS measurements of cross-sections of BMW-tested specimen.

## 4.6 GDOES CHARACTERIZATION

### 4.6.1 Investigation of the alkaline cleaning and pickling step

To investigate the influence of pickling on the steel surface composition, GDOES and XPS characterization have been carried out on 7 specimens with different surface pre-treatments. With this characterization the following aspects are investigated:

- Change of surface chemistry upon pickling.
- Preferential pickling; i.e. are some elements more likely to be etched away than other elements.
- Re-oxidation of the steel between pickling and characterization.

The first sample was not cleaned, beside an ethanol rinsing step, while all the other samples were also anodically cleaned in a sodium hydroxide bath. More details on this cleaning process are provided in section 3.3.1.

Normally, after the surface treatment step the sample is taken from the cleaning solution, dried and transported to the PVD setup for coating deposition. This can result in a re-oxidation/contamination of the surface and thereby reduce the effect of the alkaline/pickling step.

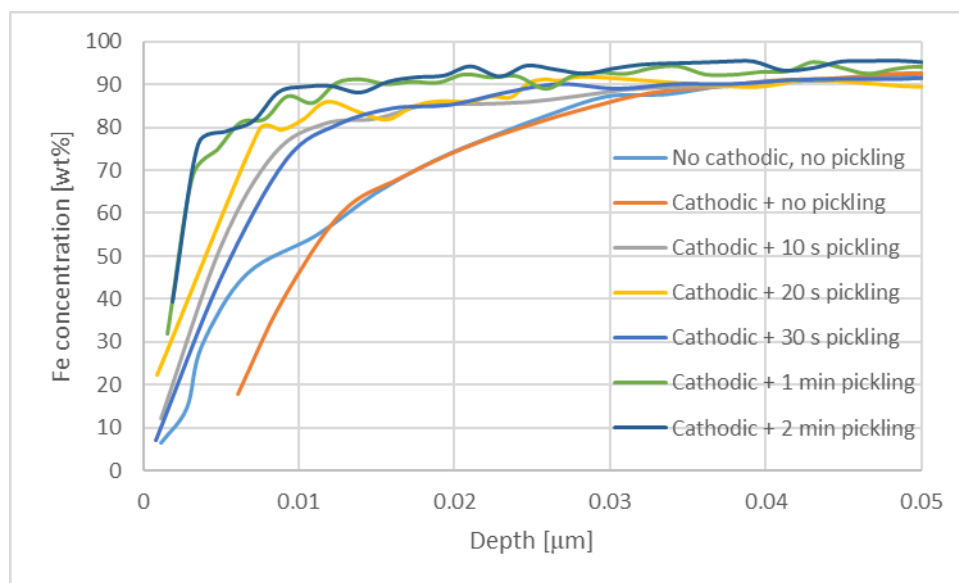


Figure 19: Iron concentration depth profile (GDOES) for different cleaning conditions

In Figure 19 the iron concentration depth profiles are shown as function of cathodic cleaning and pickling times. When no pickling is applied, then the Fe concentration reaches “bulk” values at a depth of ~30 nm. Upon pickling there is a clear shift in the iron concentration towards the surface for pickling times up to 60 s. It seems that within the first 10 nm there is always an elemental enrichment and presence of oxides, regardless the pre-treatment. This is probably caused by the transport time through ambient atmosphere where re-oxidation takes place.

Thus, without pickling the oxide and enrichment layer thickness is around 30 nm, while for pickled specimen, even after just 10 s pickling, that is ~10 nm. The original oxide thickness of the DP800 steel in the untreated state is estimated to be 30 nm, and the re-oxidation thickness is estimated to be 10 nm. As in 10 s the complete enrichment is gone, the pickling rate is estimated to be ~3 nm/s.

For the samples with pickling times of 1 and 2 minutes, the concentration curves seem to overlap, which could mean that a limit has been reached on pickling times, from where additional pickling only removes steel bulk material and the enrichment slopes are due to re-oxidation between pickling and characterization. This is in agreement with the formation of gas bubbles (hydrogen gas) after ~30 s of pickling.

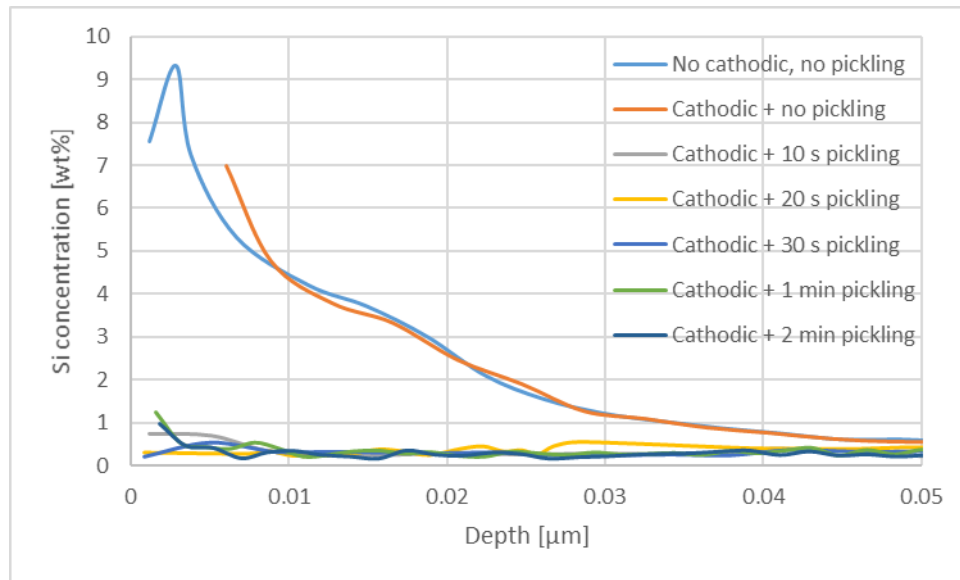


Figure 20: Silicon concentration depth profile (GDOES) for various cleaning conditions

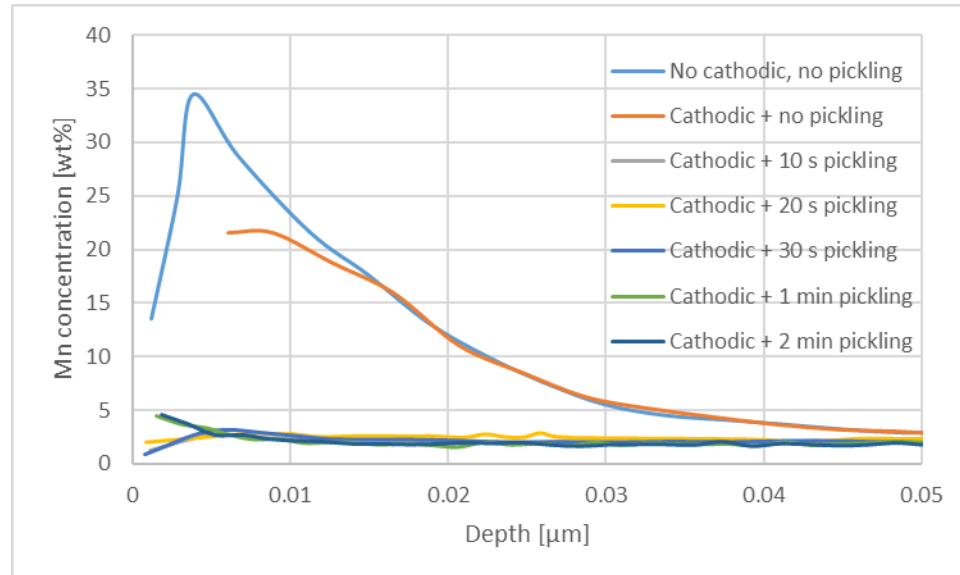


Figure 21: Manganese concentration depth profile (GDOES) for various cleaning conditions

Figures 20 and 21 show the manganese and silicon composition depth profiles as determined with GDOES. Without pickling, the concentration of both elements within the first 30 nm is relatively high.

The alkaline cleaning has a small influence on the surface concentration of manganese. However, when pickling is applied, both silicon and manganese surface enrichments are almost completely removed, even after the shortest pickling times. Surprisingly, for long pickling times there seems to be a small enrichment of manganese and silicon at the most outer surface.

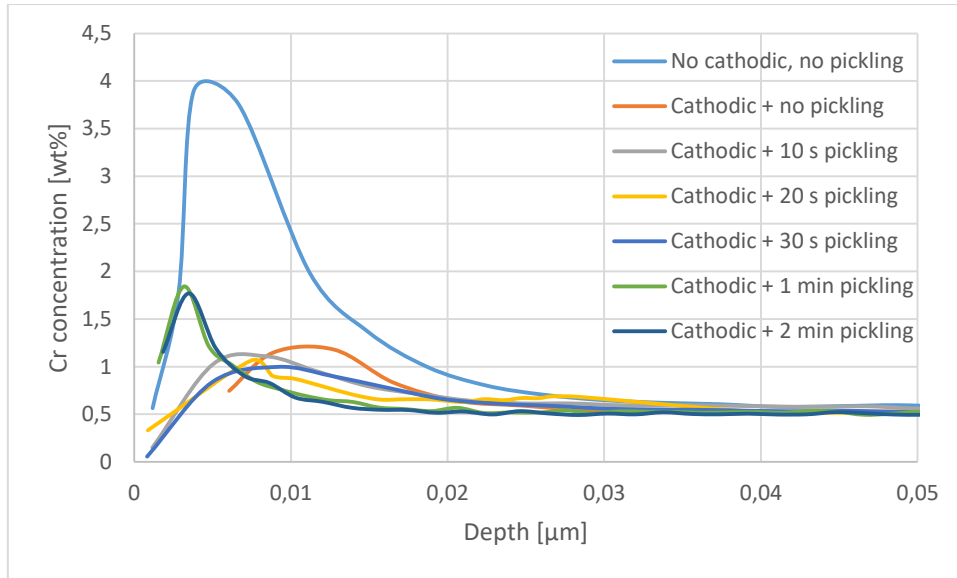


Figure 22: Chromium concentration depth profile (GDOES) for various cleaning conditions

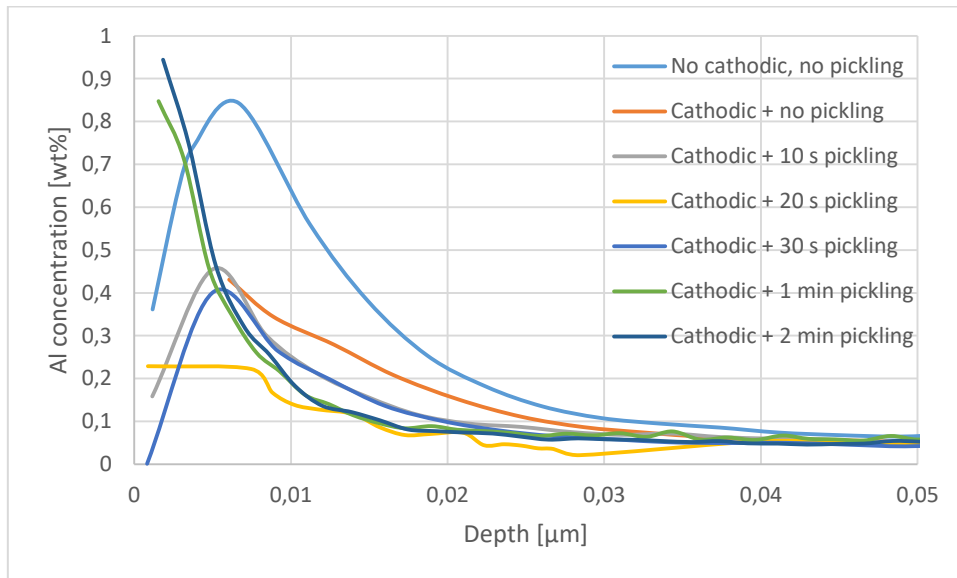


Figure 23: Aluminum concentration depth profile (GDOES) for various cleaning conditions

For chromium and aluminum, a somewhat different trend is observed as compared to manganese and silicon; see Figures 22 and 23. The enrichment of chromium (and to a lesser extent also aluminum) is already removed after the alkaline cleaning step. At longer pickling times, the same trend is observed as for manganese and silicon, i.e. at the outer surface of the sample, an enrichment of chromium and aluminum is observed.

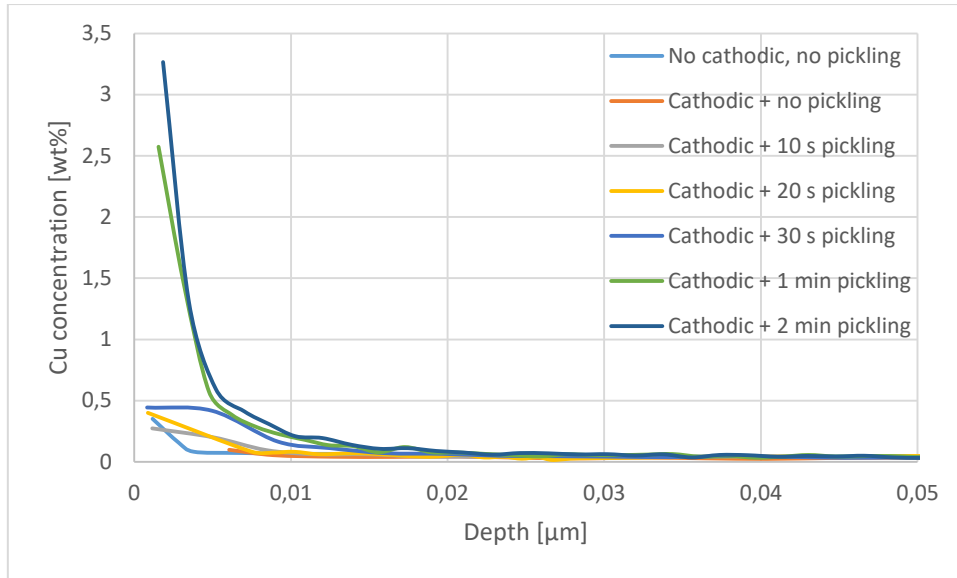


Figure 24: Copper concentration depth profile (GDOES) for various cleaning conditions

The composition depth profiles revealed the following phenomena:

- Alkaline anodic cleaning removes the chromium and aluminum enrichment at the surface, but not the silicon and manganese enrichment.
- Pickling (even for short times) removes the silicon and manganese enrichment at the surface
- After pickle times of 1 and 2 minutes, a small surface enrichment of silicon, manganese, chromium, aluminum and copper occurs.
- Pickling of 10 to 30 seconds result in the same composition near the surface.
- Pickling of 1 to 2 min result in the same composition near the surface.

#### 4.6.2 Infrared heating to improve coating adhesion

	Temperature before sputtering	Plasma sputter intensity
	°C	$\text{kJ/m}^2$
16	0	420
19	200	420
20	350	420

Table 10: Process parameters for three samples

Since the substrate temperature will become rather low for the very short sputter times, this might influence the coating adhesion properties. To get a better understanding of the influence of the substrate temperature on the coating adhesion, some tests were performed with an infrared heating lamp, as described in section 3.3.2. Three samples were prepared and characterized by GDOES. Prior to the plasma sputtering, 2 specimens were IR heated up to 200 and 350 °C, while the sputter intensities were kept constant for all three specimens; see Table 10. Then, the influence of the substrates temperature on the composition can be observed, independent of the sputter time.

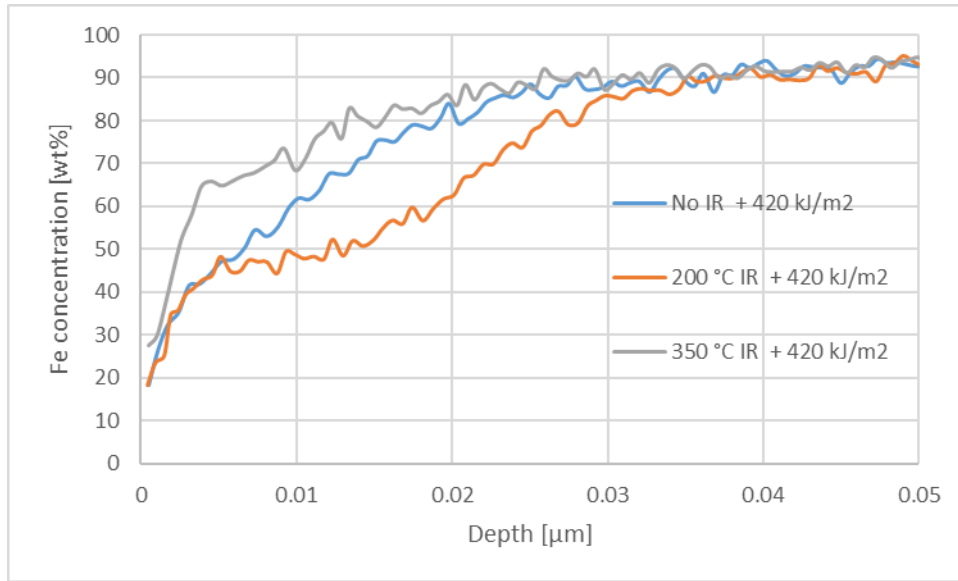


Figure 25: Iron concentration depth profile (GDOES) for various IR heating conditions

Upon heating, the iron concentration depth profile shows that the IR heating does significantly influence the composition; see Figure 25. At about 200 °C by IR heating, the iron content between 5 and 30 nm is lower than without IR heating. When heating up to 350 °C, the iron concentration seems to attain its bulk value faster.

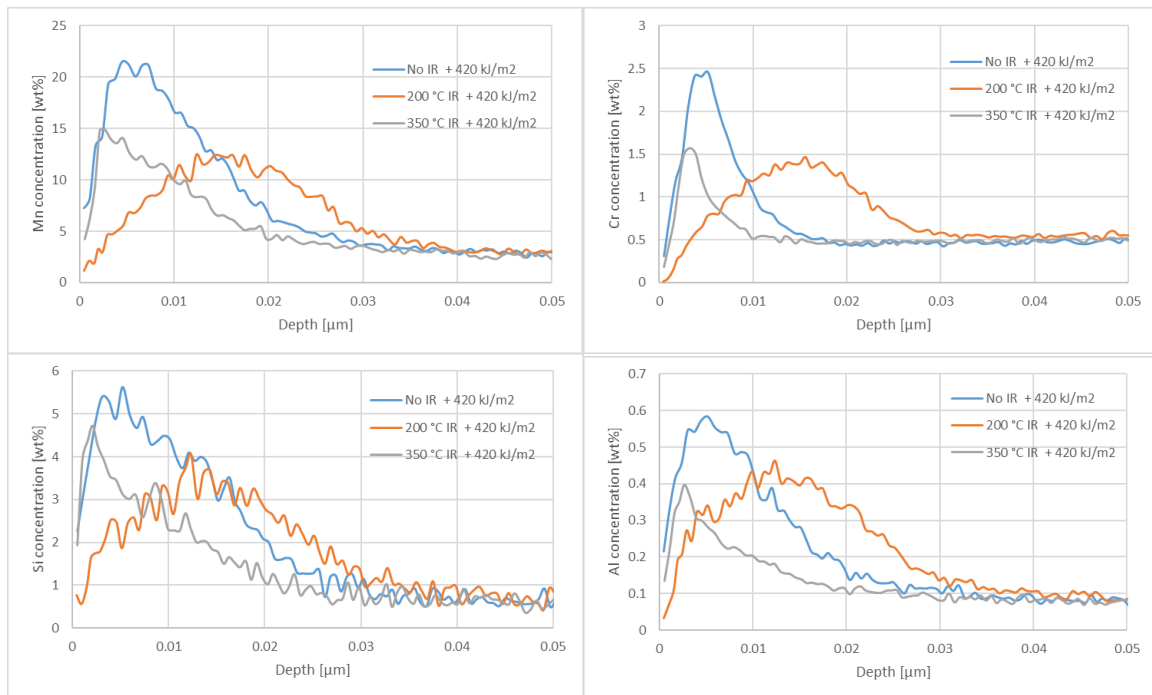


Figure 26: Manganese, chromium, aluminum and silicon (clockwise) concentration depth profiles (GDOES) for various IR heating conditions

Figure 26 shows the concentration profiles of manganese, chromium and aluminum for the samples sputtered for 2 minutes with different IR heating. It can be seen that for 200 °C the enrichment peak is somewhat lower, but more spread out over the depth of the sample; its width goes from around 20 nm up to 30 nm depth. This may be caused by faster diffusion of the alloying elements due to IR heating. When the steel is heated to 350 °C, the enrichment seems more localized to the surface.

### 4.6.3 Investigation of the plasma sputtering influence

To get a better understanding of the influence of the sputter intensity on the concentration depth profiles, specimens were plasma sputtered with different intensities. Five specimens were prepared and characterized by GDOES. The plasma sputter intensity ranged from 0 to 830 kJ/m<sup>2</sup><sup>18</sup>; see Table 10. The specimens were only cleaned by ethanol before sputtering.

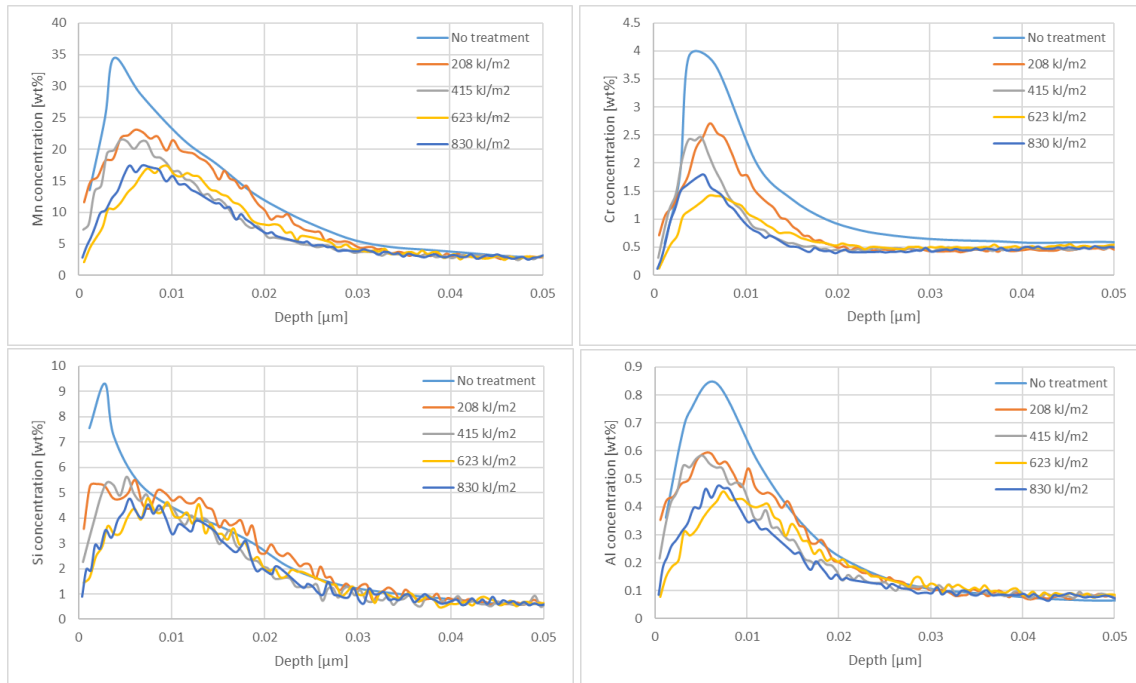


Figure 27: Manganese, chromium, aluminum and silicon (clockwise) concentration depth profiles (GDOES) for various plasma sputter conditions

It can be seen that the surface enrichments are reduced when the sputter intensity increases; see Figure 27. After 4 min of plasma sputtering still enrichment of alloying elements at the surface remained, while after pickling for even 10 s, the enrichment for these elements completely disappeared.

<sup>18</sup> 830 kJ/m<sup>2</sup> equals 4 minutes sputtering at Emely.

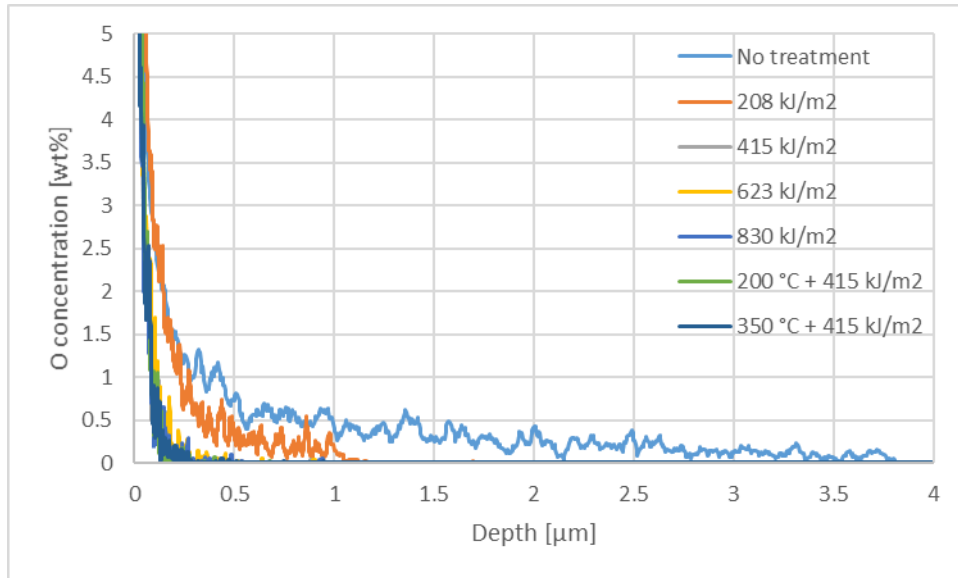


Figure 28: Oxygen concentration depth profile (GDOES) for various plasma sputter and IR heating conditions

From Figure 28 it can be seen that without sputtering there is a small oxide concentration left up to 3.8  $\mu\text{m}$  depth. For 1 minute sputtering, the oxygen is observed only up to 1  $\mu\text{m}$ . For higher sputter intensities, this oxide is completely removed from 300 nm. This indicates a clear difference between 1 minutes sputtering and 2 or more minutes sputtering.

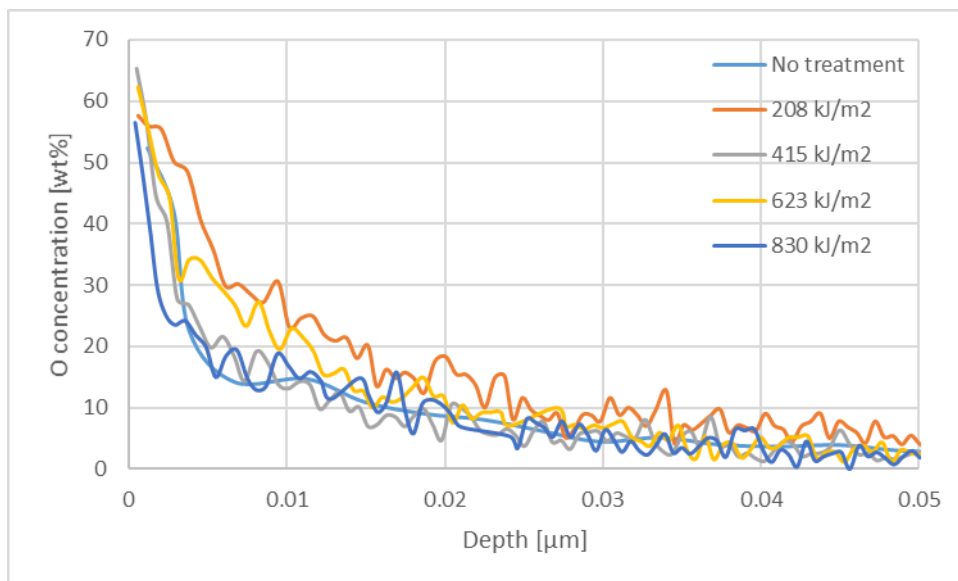


Figure 29: Oxygen concentration depth profile (GDOES) for various plasma sputter conditions

It can be seen that in the first 50 nm of the specimen there is no significant oxygen concentration difference as function of sputter time; see Figure 29. Even without sputtering the profile over the first 50 nm is similar to the profiles with sputtering. Since sputtering removes the surface layers, it is expected that the oxygen profiles over (at least) the first 50 nm is caused by re-oxidation after sputtering.

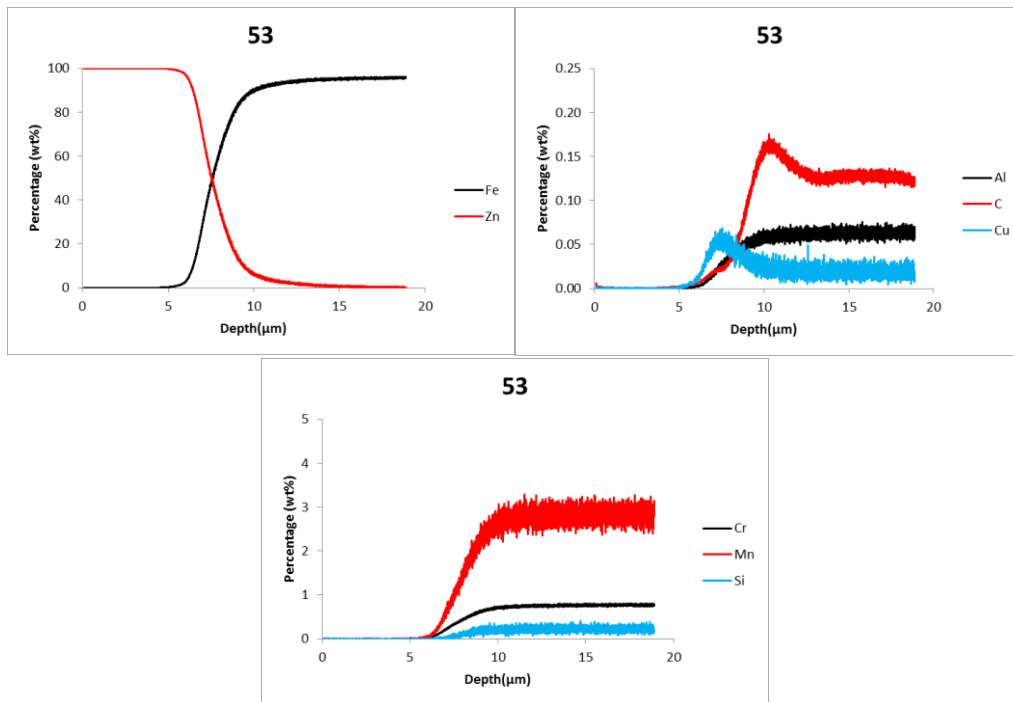


Figure 30: Concentration depth profiles (GDOES) for sample 53, various elements

In Figure 30, the concentration profile of a zinc deposited sample (nr. 53) can be seen. An enrichment of copper near the interface between steel and zinc is observed. This enrichment is probably due to sputtering of the box being made from copper. This causes re-deposition of the sputtered copper on the steel surface.

An enrichment of carbon at the interface with the zinc coating is also clearly visible; see Figure 30. This may be due to the low carbon sputter yield as calculated in Section 2.2.1.

## 4.7 XPS CHARACTERIZATION

To obtain more specific information on the outermost surface properties, XPS measurements have been performed.

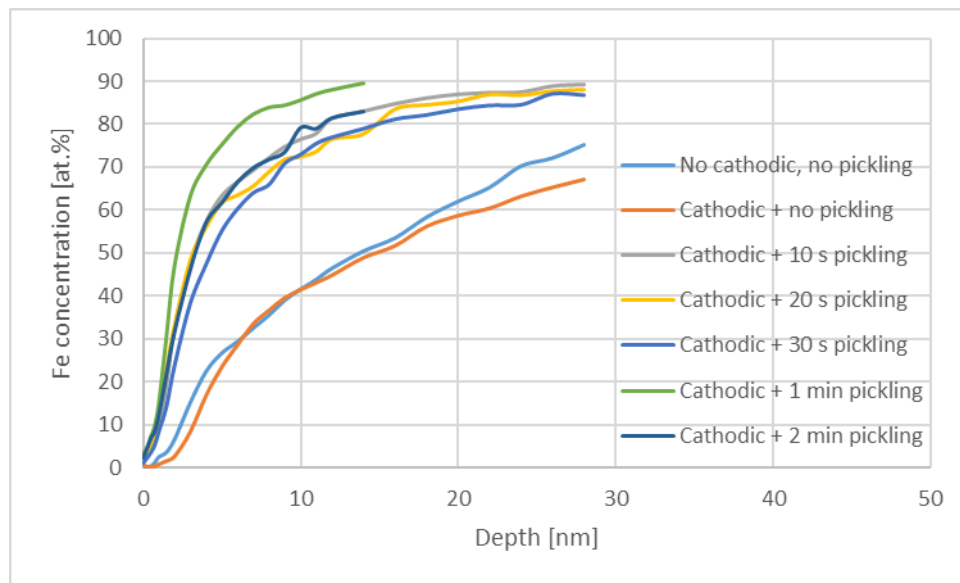


Figure 31: Iron concentration depth profile (XPS) for various cleaning regimes

In Figure 31 the iron concentration depth profiles as determined by XPS are shown as function for different pickling times. If no pickling is applied, then the iron concentration reaches “bulk” values at a depth of >30 nm, and the iron surface concentration is much lower as compared to the pickled samples. As function of pickling there is a clear shift of the iron concentration towards the surface. It seems that within the first 10-20 nm there is always an enrichment of other elements and oxides which is in agreement with the GDOES measurements. Although the results are comparable to the GDOES measurements, there is a slight shift in depth and concentration.

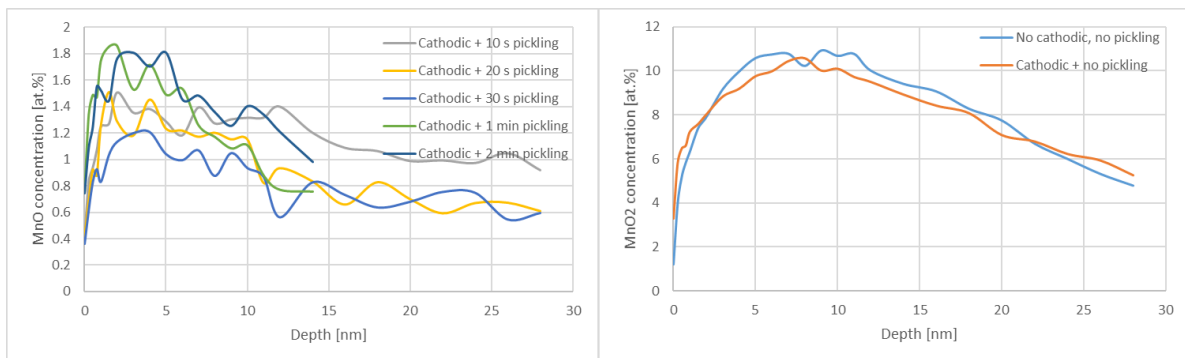


Figure 32: Manganese (di-)oxide concentration profile (XPS) for various cleaning regimes

When the steel is not pickled, manganese oxide is present in the form of  $MnO_2$ ; see Figure 32. However when pickled, the manganese oxide is only present as  $MnO$ , even up to depths of 30 nm. It is not very likely that the pickling does have a direct effect on the bulk material under the surface, unless it takes place via the grain boundaries. The change at a depth of 30 nm could therefore possibly be caused by diffusion.

From the GDOES and XPS concentration depth profiling the following observations can be made:

- Surface enrichments are typically found up to a depth of 40 nm of the untreated substrate.
- The cathodically cleaning step removes the chromium and aluminum enrichment at the surface.
- The subsequent pickling step removes most of the silicon and manganese surface enrichment even at pickling steps as short as 10 s.
- At pickling times of 1 and 2 minutes, a small enrichment seems to re-appear, for silicon, manganese, chromium, aluminum and copper.
- For the alloying elements in the surface enrichment, there does not seem to be much difference between pickling times of 10, 20 and 30 s.
- There seems not to be a difference between 1 and 2 minutes of pickling.
- It seems that at the outermost surface always some surface enrichment or oxides are present.

## 5 DISCUSSION

In this chapter four phenomena will be discussed, where obtained results and additional information will be combined.

### 5.1 INFLUENCE OF RE-OXIDATION

The influence of re-oxidation, see Section 1.3.4, seems to be an important aspect to consider within this project, since the re-oxidation in this research will be different from re-oxidation in an industrial coating line. This is due to the shorter transport times through ambient atmosphere and the possibility to do this in a protective environment.

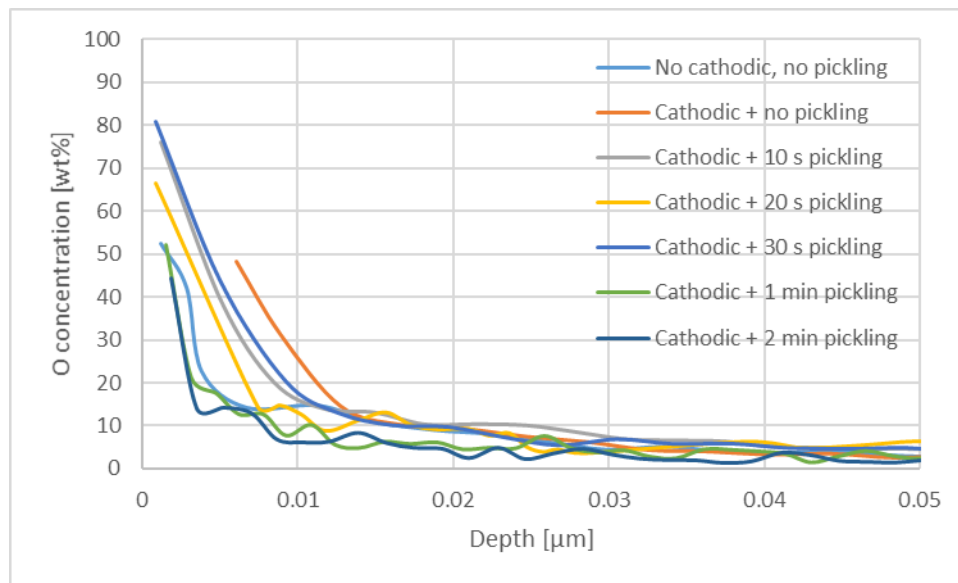


Figure 33: Oxygen concentration depth profile (GDOES) for various cleaning regimes

In Figure 33, it can be seen that increasing the pickling time can slightly lower (or enrich) the surface enrichment. But over the first 10-15 nm, there is always an increased oxygen concentration. Interestingly, this 10-15 nm thickness corresponds well to the sputter depth of the minimum required sputter intensity needed to obtain a good coating adhesion, i.e.  $420 \text{ kJ/m}^2$ ; see Section 4.1. From this observation it seems that the re-oxidation of the surface determines this minimum sputter intensity and thus depends on the transfer from the pickling setup to the PVD setup.

## 5.2 MANGANESE OXIDE

As shown in section 4.6, it seems that when the steel is not pickled, manganese oxide is present in the form of  $\text{MnO}_2$ . But whenever pickled, the manganese oxide is only present as  $\text{MnO}$ , even at depths of 30nm. It is expected that the pickling, especially for short pickling times, is not sufficient to remove the metals and oxides up to a depth in the order of tens of nm.

To know which manganese oxide formation is energetically more favorable, the Gibbs free energy of manganese oxide can be calculated. Kinetics are not involved in this calculation, it is only about which oxide is more energetically favorable to form.

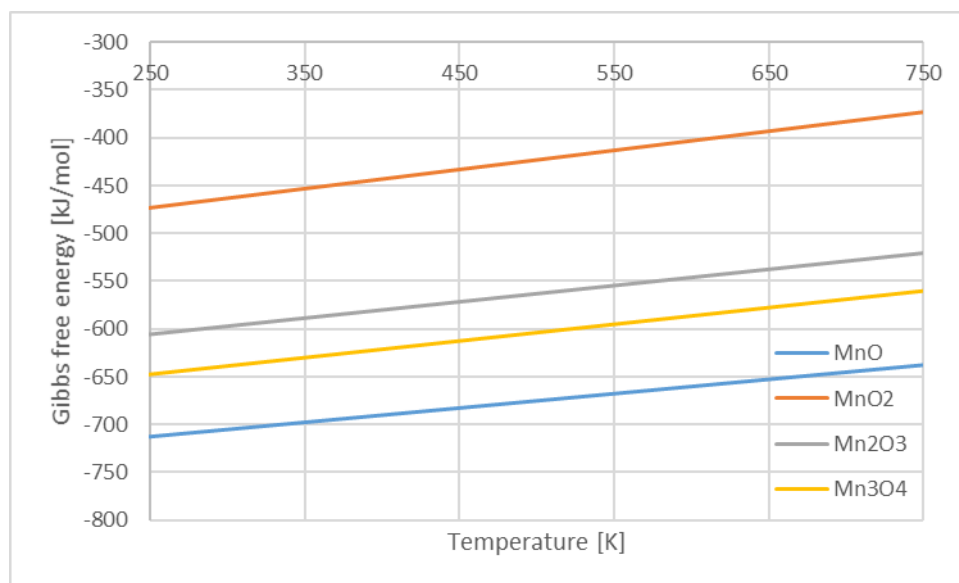
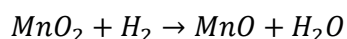


Figure 34: Calculated Gibbs free energy for various manganese oxides per mol of oxygen

In Figure 34, it can be seen that the Gibbs free energy change of  $\text{MnO}$  is lower than the other oxides, and much lower than  $\text{MnO}_2$ . So  $\text{MnO}$  is energetically more favorable to form when compared to  $\text{MnO}_2$ .

Manganese(II)oxide is commercially produced by reduction of  $\text{MnO}_2$  with (amongst others) by hydrogen gas (Reidies, 2000):



Hydrogen gas is expected as a reaction product of the pickling process, when all oxides are removed. In that circumstance, the metallic iron reacts with sulfuric acid into metal sulfate and hydrogen gas. This hydrogen gas may then react with  $\text{MnO}_2$  forming  $\text{MnO}$ . However, the bubbling was only seen after 20-30 seconds (see Section 3.3.1), which suggests that before that, there is most probably no significant hydrogen gas formation. This is in contradiction with the observation that even at 10 s pickling, there is no  $\text{MnO}_2$  observed at the surface.

### 5.3 INFLUENCE OF PLASMA SPUTTERING ON THE STEEL SURFACE STATE

It is estimated that the plasma sputtering in Emely at 200 W and a strip speed of 1 m/min has a rate between 0.15 and 0.35 nm/s (Westerwaal, Commandeur, & Bouwens, 2017). The minimum sputter time under normal conditions to achieve good adhesion is around 2 minutes (Section 4.1) which corresponds to a removed surface layer thickness between 18 and 42 nm. GDOES experiments (Section 4.6) indicate that there is always an oxygen enriched layer in the first 15 nanometers, regardless of the pre-treatment<sup>19</sup>. Therefore it is expected that with 2 minutes plasma sputtering, most of the oxide has been sputtered away.

The fact that even after 2 minutes of sputtering, coating adhesion test can fail might be related to the specific composition, oxide and structure of the steel surface. Therefore, additional sputtering removes these oxides progressively and thereby increases the adhesion strength up to the desired strength<sup>20</sup>.

From Section 2.2.1, there is a possibility that an enriched surface layer can form after plasma sputtering, due to lower sputter yields for carbon and silicon. It can be seen from the characterization in Section 4.6.3 that the composition depth profile of silicon is very similar to that of the other major alloying elements chromium and manganese. From that, it can be concluded that the difference as seen in the theoretical sputter yield is not observed in the practical plasma sputtering experiments.

---

<sup>19</sup> That is, in this project; there is always time in ambient atmosphere between pre-treatment and characterization, so re-oxidation can take place. This re-oxidation can be reduced drastically if the transport is in protected atmosphere, e.g. in a vacuum seal or submerged in isopropanol.

<sup>20</sup> Desired strength is when both the OT and BMW test results are OK, see Section 3.5.

## 5.4 COATING ADHESION INFLUENCING FACTORS

In general, it seems that pickling does only have a very limited effect on reducing the plasma sputter intensity. Furthermore, 420 kJ/m<sup>2</sup> seems to be the minimum required sputter intensity to obtain a good coating adhesion for the DP800 type of steel. This is possibly influenced by the transfer through air between the pickling and plasma sputter step, since re-oxidation takes place then. To exclude this re-oxidation, sample transfer under a protective atmosphere needs to be considered.

In contrast, research on other types of DP800 steel with a significantly higher amount of oxygen in the surface layer show a great benefit from a pickling pre-treatment. Therefore, the current obtained conclusions should be seen in that perspective; for this steel, pickling does not seem to assist the plasma sputtering in achieving good adhesion.

The morphology (Section 4.4) and the concentration profiles of the major alloying elements<sup>21</sup> (Sections 4.7 and 4.7) do not seem to be directly related to the coating adhesion strength. The oxygen concentration profile seems to be a more significant factor, mainly because:

- The minimum required sputter intensity removes around the same layer thickness as the thickness containing the high oxygen concentration in all specimens.
- Other DP800 steels also being investigated (not included in this project), do show that pickling being a useful step to reduce the plasma sputter intensity. Those steels showed a significantly higher and deeper concentration of oxygen, than the steel used in this project.
- The oxygen concentration depth profiles do not seem to change much with increasing pickling intensity. If the oxygen content is the major influence for the Zn-coating adhesion strength, this agrees with the observation that pickling does not assist the coating adhesion.

---

<sup>21</sup> That is manganese, chromium and silicon.

## 6 CONCLUSIONS

---

The minimum required sputter intensity to obtain good zinc coating adhesion is  $420 \text{ kJ/m}^2$ , irrespective of the pickling time. So the pickling does not assist the plasma sputtering in achieving good coating adhesion.

The independence of pickling suggests that there is a constant thickness of the surface needed to be removed. Assuming a plasma sputter rate of  $0.15 \text{ nm/s}$  (Westerwaal, Commandeur, & Bouwens, 2017) this corresponds to a removed surface layer thickness of  $18 \text{ nm}$ . This thickness is in the same range of the expected thickness of the formed oxide between the acid etching step and placing in the PVD installation, which was  $\sim 15 \text{ nm}$ , regardless the pickling pre-treatment. This implies that the oxide thickness can be a major influence on the coating adhesion.

Surface enrichments are typically observed up to a depth of  $40 \text{ nm}$  for this type of DP800 substrate. The alkaline cleaning step has a strong influence on the chromium and aluminum surface enrichment, but not on the iron, silicon and manganese concentrations. The pickling step is effective in removing the surface enrichment of silicon and manganese. After sputter times of more than  $2 \text{ min}$  a small re-deposition on the steel surface of silicon, manganese, chromium, aluminum and copper occurred. During pickling the surface material is removed with a rate of approximately  $3 \text{ nm/s}$ . However, during the transfer from the acid etching to the PVD installation a surface re-oxidation occurs with a thickness of about  $15 \text{ nm}$ .

The surface treatments resulting in a good zinc coating adhesion comprises at least a sputter power of  $420 \text{ kJ/m}^2$ <sup>22</sup>, which corresponds to  $13.5 \text{ nm}^2$ <sup>23</sup> of removed surface material. From Section 4.6.1 elemental enrichments up to  $300 \text{ nm}$  depth were observed, if no pickling was used. This implies that there can still be a considerable elemental enrichment at the surface while having a good coating adhesion, in the case of not-pickled specimen.

---

<sup>22</sup> It can be somewhat lower with IR heating, see Section 4.6.2.

<sup>23</sup>  $420 \text{ kJ/m}^2 = 2 \text{ min sputtering} ; 120 \text{ s} * 0.15 \text{ nm/s} = 13.5 \text{ nm}$ .

## 6.1 RECOMMENDATIONS

1. Try to minimize the re-oxidation between pickling and PVD, to get a 'cleaner' picture of the pickling influence. It is recommended to store and transport the samples in a protected environment. Such an environment could be for example isopropanol or argon gas.
2. Investigate the influence of the substrate temperature on the coating adhesion strength. Previous research saw 140 °C as the bottom limit for adhesion, but the bottom limit when combining with IR heating should also be known.
3. Investigate the cracks at the interface between the coating and the substrate; they could be caused or increased by the thermal misfit, which could be an important parameter for the adhesion strength.
4. Investigate the concentration depth profiles for pickling values between 0 and 10 seconds. Most of the change in the concentration depth profiles is between not pickling and pickling for 10 seconds.
5. If these longer pickling times/higher pickling intensities will be used in the future, it is way less time-consuming to use higher pickle bath temperatures, and thereby decrease the pickling time. It is recommended to keep the time (= strip speed) constant, but variate the acid concentration and bath temperature.

## 7 REFERENCES

---

- Bohdansky. (1980).
- Callister, W. D. (2007). *Materials Science and Engineering; an introduction*.
- Chen, F. F. (1984). *Introduction to plasma physics and controlled fusion*.
- Hillier, & Robinson. (2004). Hydrogen embrittlement of high strength steel electroplated with zinc–cobalt alloys. *Corrosion Science*, 715-727.
- Langkruis, Batyrev, Zoestbergen, Maalman, Krusemeijer, & Zwart. (2015). *Adhesion, forming and corrosion performance of dual- and triple layer coated AHSS for automotive applications, Properties with and without skin pass*.
- Langkruis, Zoestbergen, & Maalman. (2013). *Adhesion, forming and corrosion performance of multi layer Zn-Mg PVD coating systems for automotive applications*. Tata internal report 157825.
- Liebermann, M. A., & Lichtenberg, A. J. (2005). *Principles of Plasma Discharges and Materials Processing*.
- Maalman, T., Vlot, M., & Zoestbergen, E. (2011). *Staining tests PVD zinc-magnesium coatings, refsource 152255*.
- Martin, M., & Fromm, E. (1997). Low temperature oxidation of metal surfaces. *Journal of alloys and compounds*, 7-16.
- Mattox, D. M. (2001). Physical Vapor Deposition processes. *Society of Vacuum Coaters*, 409-423.
- Reidies, A. H. (2000). *Manganese Compounds*.
- Song, G. M. (2015). Evaluation of interface adhesion of hot-dipped zinc coating on TRIP steels with tensile testing and finite element calculation. *Surface effects and Contact Mechanics including Tribology*.
- Song, G. M., & Sloof, W. G. (2011). Characterization of the failure behavior of zinc coating on dual phase steel under tensile deformation. *Materials Science and Engineering*, 6432-6437.
- Song, G. M., Sloof, W. G., Pei, Y. T., & de Hosson, J. T. (2006). Interface fracture behavior of zinc coatings on steel: Experiments and finite element calculations. *Surface & Coatings Technology*, 4311-4316.
- Westerwaal, Commandeur, & Bouwens. (2017). *In house developed Ar plasma sputter system for surface preparation of steel sheets*.
- Zalm, P. C. (1984). *J. Vac. Sci. Technol.*